

Real eternal PDE solutions are not complex entire: a quadratic parabolic example

– *Dedicated to the memory of Marek Fila* –

Bernold Fiedler* and Hannes Stuke*

version of March 12, 2024

*

Institut für Mathematik
Freie Universität Berlin
Arnimallee 3
14195 Berlin, Germany

Abstract

In parabolic or hyperbolic PDEs, solutions which remain uniformly bounded for all real times $t = r \in \mathbb{R}$ are often called *PDE entire* or *eternal*. For example, consider the quadratic parabolic PDE

$$(*) \quad w_t = w_{xx} + 6w^2 - \lambda,$$

for $0 < x < \frac{1}{2}$, under Neumann boundary conditions. By its gradient-like structure, all *real eternal* non-equilibrium orbits $\Gamma(r)$ of $(*)$ are heteroclinic among equilibria $w = W_n(x)$. For parameters $\lambda > 0$, the trivial homogeneous equilibria are $W_\infty = +\sqrt{\lambda/6}$ of unstable dimension (Morse index) $i(W_\infty) = 1, 2, 3, \dots$ depending on λ , and locally asymptotically stable $W_0 = -\sqrt{\lambda/6}$. All nontrivial real W_n are rescaled and properly translated real-valued Weierstrass elliptic functions $W_n(x) = -n^2 \wp(nx + \frac{1}{2}\tau)$, $n = 1, 2, 3, \dots$, with lattice periods 1 and the purely imaginary modular parameter τ , and with Morse index $i(W_n) = n$ at $\lambda = \frac{1}{2}n^4 g_2(\tau)$.

We show that the complex time extensions $\Gamma(r + is)$, of the real analytic heteroclinic orbits towards W_0 , are *not complex entire*. For any fixed real r_0 , for example, consider the time-reversible complex-valued solution $\psi(s)$ of the nonlinear and non-conservative quadratic Schrödinger equation

$$i\psi_s = \psi_{xx} + 6\psi^2 - \lambda$$

with real initial condition $\psi_0 = \Gamma(r_0)$. Then there exist r_0 such that $\psi(s)$ blows up at some finite real times $\pm s^*$.

Abstractly, our results are formulated in the setting of analytic semigroups. They are based on Poincaré non-resonance of unstable eigenvalues at equilibria W_n , near pitchfork bifurcation. Technically, we have to except a discrete set of $\lambda > 0$, and are currently limited to unstable dimensions $n \leq 22$, or to fast unstable manifolds of dimensions $d < 1 + \frac{1}{\sqrt{2}}n$.

Contents

1	Introduction and main results	1
1.1	A paradigm	1
1.2	Semigroup setting	1
1.3	Abstract result	2
1.4	The quadratic heat equation	4
1.5	Fast unstable manifolds	6
1.6	Heat versus Schrödinger equation	7
1.7	The fastest unstable manifold	7
1.8	The quadratic ODE	10
1.9	Outline	12
1.10	Acknowledgment	12
2	Real eternal contradicts complex entire	13
3	The quadratic heat equation: Weierstrass equilibria	16
4	The quadratic heat equation: non-resonance at bifurcation	20
5	The quadratic heat equation: fast unstable manifolds	22
6	The quadratic Schrödinger equation: blow-up and blow-down	23
7	Discussion	24
7.1	Overview	24
7.2	Blow-up in sup-norm	25
7.3	ODEs revisited	26
7.4	Closure and boundaries of unstable manifolds	32
7.5	Schrödinger and parabolic singularities	34
7.6	Periodic traveling waves in complex time	38
7.7	Ultra-invisible chaos: a 1000 € question	40
7.8	Non-entire homoclinic versus entire periodic orbits	43

1 Introduction and main results

1.1 A paradigm

A major part of the work by Marek Fila and his co-authors has been dedicated to parabolic blow-up in real time. See for example the many references to his work in the standard monograph [QS19]. Interestingly, he devoted several papers to real continuation after (incomplete) real-time blow-up [FilPo99, FilMa00, FilMaPo05, FilMi07]. First attempts to circumnavigate complete real-time parabolic blow-up, by detours through complex time, go back to Kyûya Masuda [Mas82, Mas84]. In contrast, we explore blow-up in complex time, for real solutions which remain uniformly bounded, eternally, in forward and backward real time. See section 7.5 for further discussion of some available literature.

The study of finite time blow-up, for complex-valued PDEs and in complex time, is fraught with technical obstacles. Not the least among them are the absence of, both, variational structure and effective comparison principles. Specifically, the present paper explores how some heteroclinic solutions $\Gamma(t)$ of analytic semigroups, in real time $t = r$, are related to blow-up behavior, in complex time $t = r + is$. Our guiding paradigm will be:

Real eternal solutions are not complex entire.

1.2 Semigroup setting

Our abstract setting are analytic semigroups. To be specific, let $\Phi^t(w_0) := w(t)$ denote the local analytic semigroup defined by solutions $w = w(t)$ of semilinear equations

$$(1.1) \quad \dot{w} = Aw + f(w)$$

with initial condition $w(0) = w_0$. See [Hen81, Paz83] for a general background. Here the sectorial operator A is the infinitesimal generator of a linear analytic semigroup $\exp(At)$ on a complex Banach space X . The fractional power space X^α is equipped with the graph norm $\|\cdot\|_\alpha$ of the fractional power $(-A)^\alpha$. The nonlinearity $f : X^\alpha \rightarrow X$ is assumed to be *complex entire*, i.e. complex Fréchet differentiable on all X^α , for some fixed $0 \leq \alpha < 1$. We assume locally uniform bounds

$$(1.2) \quad \|f'(w)\| \leq C(\|w\|_\alpha)$$

on the derivative operators $f'(w) : X^\alpha \rightarrow X$. The local solution semigroup $\Phi^t : X^\alpha \rightarrow X^\alpha$ is then well-defined and strongly continuous, for small $|t| < \varrho(w_0)$ in a closed complex positive sector

$$(1.3) \quad \mathfrak{S}_\Theta := \{\Theta \mid |\arg t| \leq \Theta < \pi\}.$$

Complex differentiability of Φ^t holds in the interior of \mathfrak{S}_Θ . By construction, the semigroup satisfies

$$(1.4) \quad \Phi^{t_2} \circ \Phi^{t_1} = \Phi^{t_1+t_2}, \quad \Phi^0 = \text{id},$$

for all $t_1, t_2 \in \mathfrak{S}_\Theta$ such that the closed complex parallelogram $\langle t_1, t_2 \rangle$ spanned by t_1, t_2 is contained in the domain of existence of the local semiflow Φ^t .

For real times $t = r \in \mathbb{R} > 0$, let $r \in [0, r^*(w_0))$ denote the maximal interval of existence for the solution $w(r)$ of (1.1). By the locally uniform Lipschitz bound (1.2), the case $0 < r^* < \infty$ of *finite time blow-up* is then characterized by solutions $w(r)$ escaping to infinity:

$$(1.5) \quad \|w(r)\|_\alpha \rightarrow \infty \quad \text{for } r \nearrow r^* < \infty.$$

An analogous definition applies for complex times $t \rightarrow t^* = t^*(w_0)$, and t approaching t^* from any backward sector $t^* - \mathfrak{S}_\Theta$. In reverse time $r \searrow r^*$, where applicable, we sometimes speak of *finite-time blow-down*.

An *equilibrium* $W \in X^\alpha$ is a time-independent solution of (1.1), i.e.

$$(1.6) \quad 0 = AW + f(W).$$

We call W *hyperbolic* if the spectrum of the linearization $L = A + f'(W)$ at W does not intersect the imaginary axis. By [Hen81], hyperbolic equilibria W possess unique locally invariant local stable and unstable manifolds W^s and W^u in X^α which are graphs over their tangent spaces E^s, E^u at W , by the spectral decomposition $X^\alpha = E^s \oplus E^u$. They consist of all initial conditions w_0 such that, for all $\pm t \in \mathfrak{S}_\Theta$, the solution $w(t) = \Phi^t(w_0)$ exists, remains close to W , and converges to W , respectively, for $\pm \operatorname{Re} t \rightarrow +\infty$. Under our differentiability assumptions, the local invariant manifolds are complex differentiable, and hence analytic. See also [CH82].

The ODE case has been most expertly presented in [IY08]. The above properties, in the setting of analytic semigroups, mimic the ODE case very closely.

Heteroclinic solutions $\Gamma(r) \in X^\alpha$ in real time $r \in \mathbb{R}$ connect time-independent equilibria $w = W_\pm$, i.e.

$$(1.7) \quad \Gamma(r) \rightarrow W_\pm \text{ in } X^\alpha, \quad \text{for } r \rightarrow \pm\infty.$$

Depending on context, they are also called *connecting orbits*, *traveling fronts* (or backs), or *solitons*. By definition, heteroclinic orbits between hyperbolic equilibria enter the local invariant manifolds W_+^s and W_-^u at W_\pm , respectively, in real time $r \rightarrow \pm\infty$. We abbreviate heteroclinicity as $\Gamma : W_- \rightsquigarrow W_+$. Unless specified otherwise, explicitly, we subsume the *homoclinic* case $W_+ = W_-$ of non-constant $\Gamma(r)$ among the heteroclinic label.

1.3 Abstract result

Our main abstract result, in theorem 1.1 below, indicates how heteroclinic solutions $\Gamma(t)$, for real times $t = r \in \mathbb{R}$, are not complex entire, for complex $t = r + is \in \mathbb{C}$. In PDE context, solutions $\Gamma(r)$ which exist and remain uniformly bounded for all real times r are often called *eternal* or (*PDE*) *entire*. In complex analysis, unfortunately, *entire* functions are defined to be globally analytic (alias holomorphic or complex differentiable) on the whole complex plane, or on \mathbb{C}^N . To avoid confusion, we talk of *complex entire* functions,

and we avoid the term “PDE entire”, entirely. Heteroclinic solutions $\Gamma : W_- \rightsquigarrow W_+$, of course, are examples of PDE eternal solutions. In that terminology, our results on heteroclinicity will support the paradigm that real eternal solutions are not complex entire.

Spectral non-resonance of the unstable part of the linearization at the equilibrium W_- will play a crucial role in our result. In a finite-dimensional complex analytic ODE setting $X = \mathbb{C}^N$, suppose an equilibrium W possesses diagonalizable linearization $L = A + f'(W)$ and spectrum $\text{spec } L = \{\mu_0, \dots, \mu_k\}$. We call W *spectrally resonant*, if there exists a nonnegative integer multi-index $\mathbf{m} = (m_0, \dots, m_k)$ of order $|\mathbf{m}| := m_0 + \dots + m_k \geq 2$, such that

$$(1.8) \quad \mu_j = \mathbf{m} \cdot \mu := m_0\mu_0 + \dots + m_k\mu_k$$

holds, for some μ_j . Else, we call W *non-resonant*. For analytic semigroups we apply the same terminology to finite unstable spectrum.

We are now ready to state our main result: the exclusion of complex entire heteroclinic orbits $\Gamma(t) : W_- \rightsquigarrow W_+$.

1.1 Theorem. *In the above complex analytic setting, assume*

- (i) $\Gamma : W_- \rightsquigarrow W_+$ *is heteroclinic between hyperbolic equilibria W_{\pm} in real time $t = r \in \mathbb{R}$;*
- (ii) *the target equilibrium W_+ is linearly asymptotically stable in real time $t = r \geq 0$;*
- (iii) *the local unstable manifold W_-^u of W_- is finite-dimensional;*
- (iv) *the linearization at W_- within W_-^u is diagonalizable, with real non-resonant unstable spectrum.*

Then $\Gamma(t)$ cannot possess any complex entire time extension to all $t = r + is \in \mathbb{C}$.

To our knowledge, such a link has first been established in a PDE context in the dissertation thesis [Stu17, Stu18]. A much less explicit foreboding, in the different and very restrictive setting of complex entire planar diffeomorphisms, can be attributed to Ushiki [Ush80]. See also [Ush81] for the special heteroclinic case $i(W_-) = 1$, $i(W_+) = N - 1$ in higher finite dimensions N . Section 7.5 is dedicated to a more detailed discussion of the literature. For a more detailed survey of the ODE case, we refer to our recent survey in [Fie23], and to the discussion sections 7.7, 7.8 below.

The significance of non-resonance lies in *Poincaré’s theorem on analytic linearization*; see [IY08] for a complete proof. See further comments in section 2, where we prove theorem 1.1.

Unstable targets W_+ are admissible, if Γ emanates from the one-dimensional fastest unstable manifold of W_- . See corollary 1.5 in section 1.7 below.

In the ODE case $X = \mathbb{C}^N$, heteroclinic orbits $\Gamma : W_- \rightsquigarrow W_+$ to unstable hyperbolic targets W_+ are admissible, in complete generality. We still assume real non-resonant spectrum in the unstable and fast unstable manifolds at W_- . At the target W_+ , we also have to

assume that the stable spectrum is real and, among itself, non-resonant. See [Fie23] for details. In the PDE case, however, infinite-dimensional non-resonance at W^+ cannot be brought to bear, because Poincaré linearization is unavailable in infinite dimensions.

1.4 The quadratic heat equation

Our main example is the quadratic parabolic PDE

$$(1.9) \quad w_t = w_{xx} + 6w^2 - \lambda.$$

Indices indicate partial derivatives. We consider $0 < x < \frac{1}{2}$, under Neumann boundary conditions, and assume real parameters $\lambda > 0$. Note how any real or complex solution $w = w(t, x)$, at parameter λ , rescales to solutions

$$(1.10) \quad w_n = n^2 w(n^2 t, nx), \quad \lambda_n = n^4 \lambda,$$

for integer $n = 1, 2, 3, \dots$ and at rescaled parameters λ_n .

Consider real solutions w for real time $t = r$. Scalar parabolic PDEs in one space dimension possess a gradient-like structure, in great generality. See [Lap22, Lap23], most recently, and the many earlier references there. By the gradient-like structure, all non-equilibrium eternal solutions $\Gamma(r)$ of (1.9) are then heteroclinic among real equilibria $w = W_n(x)$. The two trivial homogeneous equilibria are $W_\infty = \sqrt{\lambda/6}$ and $W_0 = -\sqrt{\lambda/6}$. All nontrivial equilibria $W = W(x)$ are non-constant solutions of the equilibrium ODE

$$(1.11) \quad 0 = W_{xx} + 6W^2 - \lambda.$$

Therefore, they are real-valued *Weierstrass elliptic functions* $-\wp(z)$, properly translated, and scaled according to (1.10). See [Akh90, Fri1916, Lan87, Lam09] for some background, including standard notation. The functions $\wp(z)$ are meromorphic and doubly periodic in $z \in \mathbb{C}$. Their period lattice is generated by $1, \tau$ with $\text{Im } \tau > 0$. In our case, $W_n(x) = -n^2 \wp(nx + \frac{1}{2}\tau)$ or $-n^2 \wp(nx + \frac{1}{2} + \frac{1}{2}\tau)$, at $\lambda = \frac{1}{2}n^4 g_2(\tau)$, are real, of Morse indices (alias unstable dimensions) $i(W_n) = n$. See section 3 for details.

The analytic semigroup setting for (1.9) is standard: $A := \partial_{xx}$, $X = L^2$, and $X^{1/2} = H^1 = W^{1,2}$ with the H^1 -norm $\|w_0\|_{H^1}^2 := \|w_0\|_{L^2}^2 + \|\partial_x w_0\|_{L^2}^2$. Any complex sector $t \in \mathfrak{S}_\Theta$ with opening angle $0 < \Theta < \pi/2$ is admissible for the semigroup. The analytic nonlinearity $f : H^1 \rightarrow L^2$ is induced by the polynomial $f(w) := 6w^2 + 1 - \lambda$. As a technical consequence of this setting, the present paper addresses blow-up in H^1 . For L^∞ blow-up, see our comments in section 7.2.

Note that the resolvent of A is compact. Hence, unstable manifolds are automatically finite-dimensional. By standard Sturm-Liouville theory, the L^2 -selfadjoint linearization $L = A + f'(W)$ at any real equilibrium W possesses simple real spectrum

$$(1.12) \quad \mu_0 > \mu_1 > \dots \searrow -\infty$$

with L^2 -complete orthonormal eigenfunctions $\varphi_0, \varphi_1, \dots$; see also (4.1), (4.2) below. Hyperbolic $W = W_n$ of Morse index $n = i(W)$ are characterized by $\mu_{n-1} > 0 > \mu_n$.

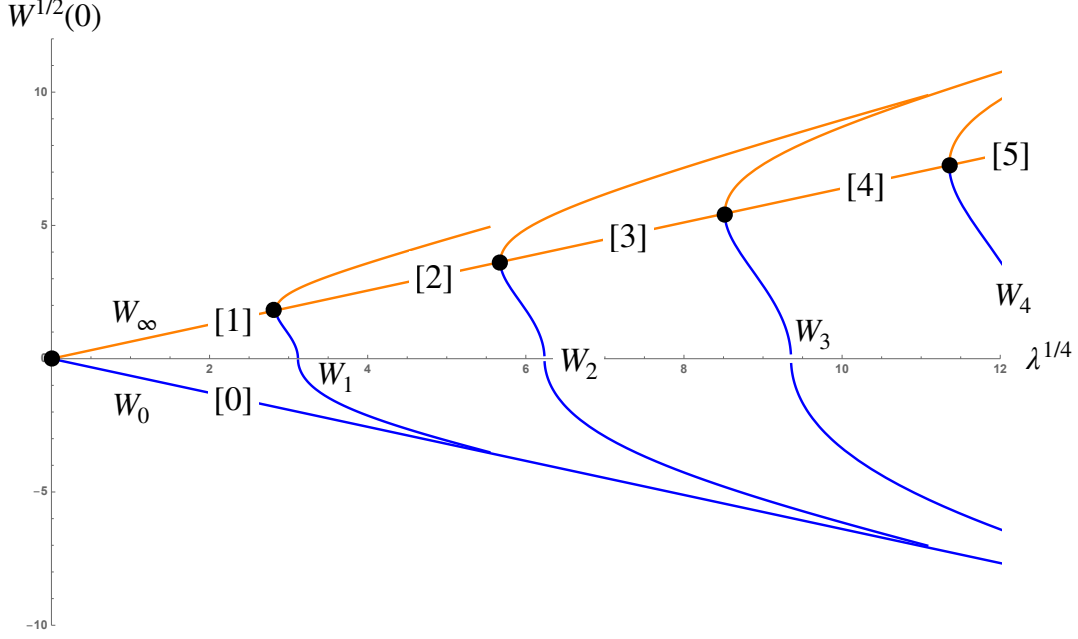


Figure 1.1: Bifurcation diagram of equilibria W_n for the quadratic heat equation (1.9), (1.11) and parameters $\lambda > 0$. The horizontal axis $\lambda^{1/4}$ and the vertical axis of signed roots $W^{1/2}(0)$ render the equilibrium scaling (1.10) as stretching by a factor n . Morse indices $i(W)$ are indicated in brackets $[\cdot]$, for $W = W_0, W_\infty$. Note how W_0 (blue) is the unique asymptotically stable equilibrium. Black dots mark bifurcations. The saddle node bifurcation of the trivial spatially homogeneous branches W_0, W_∞ occurs at $\lambda = W = 0$, and is rendered as a wedge. The remaining bifurcations are supercritical pitchforks of branches W_n with Morse index $i = n$, emanating from W_∞ (orange) at $\lambda = \frac{2}{3}(n\pi)^4$ with successively higher unstable dimensions; see (1.14). The upper branches $W_n(0) = -n^2 e_2$ (orange) and the lower branches $W_n(0) = -n^2 e_3$ (blue) are related by a half-period shift in x . The vertical tangents at $W_n(0) = 0$ (blue) are an artifact of axis scaling, and do not indicate linear degeneracy.

Real heteroclinic orbits have been studied in much detail and generality, for decades, starting with Chafee and Infante [ChIn74], and many others. For some results and surveys on general dissipative nonlinearities $f(w)(x) = g(x, w, w_x)$ see [Ra02, FieRo23a, FieRo24] and the many references there. In addition to the gradient-like structure mentioned above, intersection and nodal properties like the zero number play an essential role here. The results apply, in particular, to cubic dissipative regularizations $g^\varepsilon(w) := 6w^2 - \lambda - \varepsilon w^3$ of (1.9). For $\varepsilon > 0$, dissipativeness implies that the global attractors \mathcal{A}^ε consist of precisely all eternal solutions. By the gradient-like structure, the global attractors decompose into equilibria and heteroclinic orbits among them. For general background on global attractors, see [ChVi02, Ha88, HaMO02, Lad91, Tem88].

The global attractors \mathcal{A}^ε of the dissipative regularizations are all C^0 orbit equivalent to the standard and celebrated Chafee-Infante attractors. In the limit $\varepsilon \searrow 0$, the largest positive homogeneous equilibrium escapes to $+\infty$. The remaining set of eternal solutions, at $\varepsilon = 0$, is bounded. In fact, for any two hyperbolic equilibria W_\pm with Morse indices $i(W_\pm)$, we encounter heteroclinic orbits

$$(1.13) \quad \Gamma : W_- \rightsquigarrow W_+ \quad \Leftrightarrow \quad i(W_-) > i(W_+).$$

This is quite analogous to the dissipative Chafee-Infante case, except for those orbits in the

unstable manifolds W_-^u which blow up in finite real time. For a result on prescribed sign-changing profiles at real-time blow-up, which involves nodal properties, see [FieMa07]. We omit further details, because these constructions are not a main aspect of our present paper.

Instead, we focus on blow-up in complex time. Based on theorem 1.1, we obtain the following result.

1.2 Theorem. *In the bifurcation diagram of figure 1.1, consider heteroclinic orbits (1.13) for hyperbolic source equilibria W_- along any branch W_n , for $1 \leq n \leq 22$, or along W_∞ . Then unstable spectral non-resonance holds at most W_- . More precisely, unstable spectral resonance (1.8) along W_n only occurs at a discrete set of resonant parameters $\lambda \geq 0$. For spatially homogeneous $W_- = W_\infty$, spectrally resonant parameters do in fact accumulate, from above, at the points*

$$(1.14) \quad \lambda_{n0} := \frac{2}{3}(n\pi)^4, \quad n = 1, 2, 3, \dots$$

of pitchfork bifurcations, but no restriction to $1 \leq n \leq 22$ is imposed.

In particular, $\Gamma : W_- \rightsquigarrow W_0$ at nonresonant parameters cannot possess any entire time extension to all complex $t = r + is \in \mathbb{C}$.

1.5 Fast unstable manifolds

A variant of theorem 1.2 addresses local *fast unstable manifolds* W_-^{uu} at the equilibrium $W_- = W_n$. These locally invariant submanifolds of dimension $d < n$ are uniquely characterized by asymptotic decay of exponential rates faster than $\mu_d > 0$, in real time $r \rightarrow -\infty$. They are therefore tangent to the span of the associated eigenfunctions $\varphi_0, \dots, \varphi_{d-1}$. Like the local unstable manifold W_-^u itself, the fast unstable manifolds W_-^{uu} are complex analytic in a neighborhood of W_- .

1.3 Theorem. *In the setting of theorem 1.2 and figure 1.1, assume the heteroclinic orbit $\Gamma : W_- \rightsquigarrow W_0$ emanates from W_- via the local fast unstable manifold W_-^{uu} of dimension $d < n := i(W_-)$. Assume*

$$(1.15) \quad d < 1 + \frac{1}{\sqrt{2}} n.$$

Then unstable spectral non-resonance within W_-^{uu} holds at most W_- . I.e., unstable spectral resonance (1.8) occurs at a discrete set of parameters $\lambda \geq 0$, at most. This holds for all d, n , all $W = W_n$, and includes the case $W = W_\infty$, without any exceptional accumulations at the bifurcation values (1.14) in the latter case.

In particular, $\Gamma : W_- \rightsquigarrow W_0$ cannot possess any complex entire extension to all complex times $t = r + is \in \mathbb{C}$.

At bifurcation, the non-resonance bound (1.15) is optimal, asymptotically for large n ; see (5.3) in the proof section 5 below.

1.6 Heat versus Schrödinger equation

Given heteroclinic orbits $\Gamma(t)$ as in the theorems above, which are real analytic but not complex entire, let $\psi(s) := \Gamma(r_0 - is)$ track complex time extensions $\Gamma(t)$ in the imaginary time direction, for fixed real r_0 . Then $\psi(s) \in H^1$ solves the nonlinear and nonconservative Schrödinger equation

$$(1.16) \quad i\psi_s = \psi_{xx} + 6\psi^2 - \lambda.$$

The solutions of (1.16) define a strongly continuous (but not analytic) local semigroup $\psi(s) = S^s\psi_0$ in H^1 [Paz83, Tan79]. We can still define *blow-up* as

$$(1.17) \quad \|\psi(s)\|_{H^1} \rightarrow \infty \quad \text{for } s \nearrow s^* \text{ and } s \searrow -s^*,$$

at some finite positive s^* .

Note *time reversibility* of (1.16) here, under complex conjugation $\psi \mapsto \bar{\psi}$. Indeed, $\psi(s)$ is a solution, if and only if $\bar{\psi}(-s)$ is. In other words, the strongly continuous local solution semigroup S^s satisfies

$$(1.18) \quad S^s(\bar{\psi}_0) = \overline{S^{-s}(\psi_0)}.$$

In particular, we have a strongly continuous local solution *group* S^s , for the Schrödinger equation (1.16).

1.4 Theorem. *Under the assumptions of theorems 1.2 or 1.3, there exists a real initial condition $\psi_0 = \Gamma(r_0)$ for the Schrödinger equation (1.16), such that the solution $\psi(s)$ blows up at some finite real time $s^* > 0$ and, correspondingly, blows down from $-s^* < 0$.*

1.7 The fastest unstable manifold

The case of the *fastest unstable manifold* W_-^{uu} of dimension $d = 1$ is particularly intriguing. Under Dirichlet boundary conditions, it has already been addressed in [Stu17, Stu18]. We elaborate on the spatially homogeneous Neumann case $W_- = W_\infty$ in the next section 1.8.

For one-dimensional W_-^{uu} , we can drop any stability assumption on the target W_+ , in the semigroup setting of theorem 1.1. By [BrFie86], a heteroclinic orbit $\Gamma(r)$ emanates from the fastest unstable manifold W_-^{uu} of dimension $d = 1$, at W_- , if and only if $\Gamma(r)$ becomes tangent to the eigenvector φ_0 of the (unique) fastest unstable eigenvalue μ_0 , for $r \searrow -\infty$.

1.5 Corollary. *In the analytic semigroup setting of section 1.2, assume*

- (i) $\Gamma : W_- \rightsquigarrow W_+$ is heteroclinic between hyperbolic equilibria W_\pm in real time $t = r \in \mathbb{R}$;
- (ii) the unstable eigenvalue μ_0 of largest real part, at W_- , is unique, real, and algebraically simple;
- (iii) $\Gamma(r)$ is tangent to φ_0 , at W_- .

Then $\Gamma(t)$ cannot possess any complex entire time extension to all $t = r + is \in \mathbb{C}$.

In particular, theorems 1.3, 1.4 remain valid under these modified assumptions.

Proof. We will eventually suppose $t \mapsto \Gamma(t)$ is complex entire, and obtain a contradiction. For the moment, we proceed without this indirect extra assumption.

The simple eigenvalue μ_0 alone cannot be resonant; see (1.8). Local Poincaré linearization in W_-^{uu} at W_- therefore implies periodicity

$$(1.19) \quad \Gamma(t + ip) = \Gamma(t)$$

for all $t = r + is \in \mathbb{C}$ with, say, $r \leq 0$. For details see (2.3) below. Here $p = 2\pi/\mu_0$ is the minimal period in the imaginary time direction. At fixed s , let $-\infty < r < r^*(s) \in (0, +\infty]$ denote the maximal interval of existence for $\Gamma(r + is)$, in real time r . Define the analyticity region

$$(1.20) \quad \mathcal{D} := \{r + is \mid -\infty < r < r^*(s)\}$$

by the semigroup solution of (1.1), alias analytic continuation, in real time.

We now invoke our indirect assumption that Γ is complex entire, i.e. $\mathcal{D} = \mathbb{C}$. We claim

$$(1.21) \quad \Gamma(r + is) \rightarrow W_{\pm} \quad \text{for} \quad r \rightarrow \pm\infty.$$

For $r \searrow -\infty$, convergence follows from linearization (2.3). For $r \nearrow +\infty$, the locally s -uniform limit $\Gamma(r + is) \rightarrow W_+ = W_0$ follows from commutativity (1.4) in sectors.

In particular, (1.21) implies that Γ is uniformly bounded, hence constant by Liouville's theorem. This proves the corollary, in the semigroup setting.

For the quadratic heat and Schrödinger equations, (1.9) and (1.16), we show below that the target W_+ necessarily coincides with the only asymptotically stable equilibrium W_0 . Therefore theorems 1.3 and 1.4 apply directly, as stated. \bowtie

Let us now return to the quadratic heat equation (1.9). Originating from spatially non-homogeneous $W_- = W_n$, the fastest real heteroclinic orbits Γ are spatially non-homogeneous. Indeed, they emanate from W_- , tangentially along the eigenfunction $-\varphi_0 < 0$ of the largest Sturm-Liouville eigenvalue $\mu_0 > 0$. By [BrFie86], the real heteroclinic orbit $\Gamma : W_n \rightsquigarrow W_+$ must decrease monotonically to its target equilibrium $W_+ < W_-$. In fact, $\Gamma_r < 0$ for all real times r . Monotone convergence to W_+ implies convergence tangent to φ_{+0} , the positive eigenfunction of the largest eigenvalue μ_{+0} at W_+ . Therefore $\mu_{+0} < 0$, and the hyperbolic target W_+ is an asymptotically stable equilibrium. This observation applies to general nonlinearities $f(w)(x) = g(x, w(x), w_x(x))$ in (1.1), (1.9). In our quadratic case (1.9), it identifies $W_+ = W_0$ as the lower homogeneous equilibrium.

For $f(w)(x) = g(w(x))$, we can alternatively invoke phase plane analysis of $(W, W_x) \in \mathbb{R}^2$, as in [BrFie88, BrFie89, FieRoW11, FieRo14]. Spatially non-homogeneous real Neumann equilibria W_{\pm} of (1.1) are then parts of non-constant, x -periodic orbits of the Hamiltonian

pendulum $W_{xx} + g(W) = 0$. Such orbits are excluded as target options W_+ , because they would have to be nested with W_- , in the real phase plane, rather than located below W_- in \mathbb{R} . Therefore, the target W_+ coincides with the largest spatially homogeneous equilibrium $g(W) = 0$ below W_- . In our quadratic case, this equilibrium is $W_+ = W_0$ again.

We can identify some blow-up, more specifically. Together with reversibility (1.18), periodicity (1.19) implies that $\Gamma(r + is)$ is real (for all x), if and only if

$$(1.22) \quad s \equiv 0 \quad \text{or} \quad s \equiv p/2 \pmod{p}.$$

The real orbit $w(r) = \Gamma(r + ip/2)$ emanates from $W_- = W_n$, tangentially to the eigenfunction $+\varphi_0 > 0$. It is therefore monotonically increasing with r , rather than decreasing. Let $r \in (-\infty, r^*)$ denote the maximal interval of existence. In absence of any equilibrium $W > W_n$, we have

$$(1.23) \quad \|w(r)\|_{H^1} \rightarrow \infty \quad \text{for} \quad r \nearrow r^*(p/2) \leq \infty.$$

The comparison principle can then be invoked to show finite time blow-up $r^*(p/2) < \infty$, in the sense of (1.5), rather than grow-up $r^*(p/2) = \infty$.

Next consider Schrödinger blow-up in (1.16) for solutions $\psi(s) = \Gamma(r_0 + is)$ starting from some suitable $\psi_0 = \Gamma(r_0)$ on that fastest real heteroclinic orbit $\Gamma : W_n \rightsquigarrow \Gamma_0$; see theorem 1.4. By periodicity (1.19), reversibility (1.18), and because $\Gamma(\mathbb{R})$ is real, the boundary $s \mapsto r^*(s) \leq +\infty$ of the analyticity region \mathcal{D} in (1.20) is p -periodic and symmetric:

$$(1.24) \quad r^*(s + p) = r^*(s) \quad \text{and} \quad r^*(p - s) = r^*(s),$$

for all $s \in \mathbb{R}$. Since $\mathcal{D} \subsetneq \mathbb{C}$, the lower semicontinuous boundary $r^*(s) \not\equiv +\infty$ attains its finite minimum r_0 at some minimal $s_0 > 0$. Note $0 < s_0 \leq p/2$, by symmetry (1.24) and minimality of s_0 . Moreover $r^*(s_0) = r_0$, and $s^*(r_0) = s_0 \leq p/2$ is the positive Schrödinger blow-up time of $\psi(s)$, starting from $\psi_0 = \Gamma(r_0)$. For details on this last step, see our proof of theorem 1.4 in section 6 and, in particular, the discussion of the rectangle \mathcal{R} with upper right corner $r_0 + is_0$ in (6.1).

As a caveat, we add that we have *not* excluded Schrödinger blow-up times $p/2 < s^*(r) < +\infty$, for other $\psi_0 = \Gamma(r)$ and $r > r_0$. However, reversibility then implies violation $\psi(p/2) \neq \psi(-p/2)$ of p -periodicity, at nonvanishing imaginary part. This would be reminiscent of Masuda's discrepancy [Mas82, Mas84] between upper and lower complex detours around real-time blow-up. See section 7.5 for further discussion.

As a peculiarity of dimension $d = 1$, and an advantage of our complex viewpoint, we now understand how fastest real heteroclinicity $\Gamma : W_n \rightsquigarrow W_0$, at imaginary level $s = 0$, and real blow-up, at imaginary level $s = p/2 = \pi/\mu_0$, are just two aspects of one and the same underlying complex fastest unstable manifold W^{uu} . Indeed, the two phenomena are contingently related, half a period apart, in the foliation by fixed imaginary times is , $s \pmod{p}$. In s , the bounded fastest heteroclinic orbit Γ also provides real initial conditions $\psi_0 = \Gamma(r_0)$ for complex Schrödinger blow-up of $\psi(s)$ at times $\pm s^*$ not exceeding the half-period $p/2$. We will return to a more global viewpoint of the fastest unstable manifold,

and continuation beyond the analyticity region \mathcal{D} , in discussion sections 7.3 on spatially homogenous ODE solutions, and in 7.4 on the closure and boundary of unstable manifolds. See also figure 1.2 and the next section.

1.8 The quadratic ODE

Even in the most elementary ODE case $\dot{w} = 6w^2 - \lambda$ of spatially homogeneous solutions, it is instructive to see these results at work; see figure 1.2. In complex notation and real time $t = r$, the associated spatially homogeneous equations (1.9) and (1.16) then read

$$(1.25) \quad w_r = w^2 - 1,$$

$$(1.26) \quad i\psi_s = \psi^2 - 1.$$

Here we have first rescaled w to the case $\lambda = 6$, and then rescaled real time appropriately. Other complex quadratic vector fields can be rescaled, similarly, up to a complex rescaling of time and the purely quadratic case $\lambda = 0$. For $w = u + iv$ we obtain the equivalent real system

$$(1.27) \quad \begin{aligned} \dot{u} &= u^2 - v^2 - 1, \\ \dot{v} &= 2uv. \end{aligned}$$

The equilibria are the attractor $W_0 = -1$ (blue dot) and the repeller $W_\infty = +1$ (red dot). All nonstationary orbits (blue) are heteroclinic $\Gamma : W_\infty \rightsquigarrow W_0$. The real u -axis $\{v = 0\}$ is invariant and contains the monotonically decreasing heteroclinic orbit $u_0 : 1 \rightsquigarrow -1$. The two unbounded real orbits u_∞ on the u -axis (cyan) look like an exception, at first: they blow up at $u = \pm\infty$ in finite positive or negative time.

Unlike the general PDE case of $W_- = W_n$, the ODE (1.25) can be regularized on the Riemann sphere \mathbb{C}_∞ . Just note equivariance of $\dot{w} = w^2 - 1$ under the involution $w \mapsto 1/w$. In particular, the two blow-up pieces of u_∞ can be joined to indicate yet another single heteroclinic orbit, in the Riemann sphere. Indeed, u_∞ is just the involutive copy of u_0 , in \mathbb{C}_∞ .

Because $\dim w = 1$, Poincaré linearization near $W_\infty = 1$ shows that the complex heteroclinic orbit Γ is periodic of minimal period $p = \pi$ in imaginary time. In other words, the meromorphic heteroclinic orbit $t \mapsto \Gamma(t)$ provides a bi-holomorphic map between complex cylinders,

$$(1.28) \quad \Gamma : \mathbb{C}/\pi i\mathbb{Z} \rightarrow \mathbb{C}_\infty \setminus \{\pm 1\}.$$

By corollary 1.4, blow-up to $\psi(s) = \infty$ must occur, for some $r = r_0$ and at some $s = s^*$. Bi-holomorphy (1.28) implies that r_0 and s^* are unique. Here real $\Gamma(r) := u_0(r) \in (-1, 1)$ has to track the bounded decreasing real heteroclinic orbit. By time reversibility (1.18) of (1.16) in s , blow-up must therefore occur at

$$(1.29) \quad s^* \equiv \pi/2 \pmod{\pi},$$

for some $\psi_0 = \Gamma(r_0)$. Also, $\Gamma(r \pm \pi i/2) \in \mathbb{R}$, except at the blow-up point $r = r_0$.

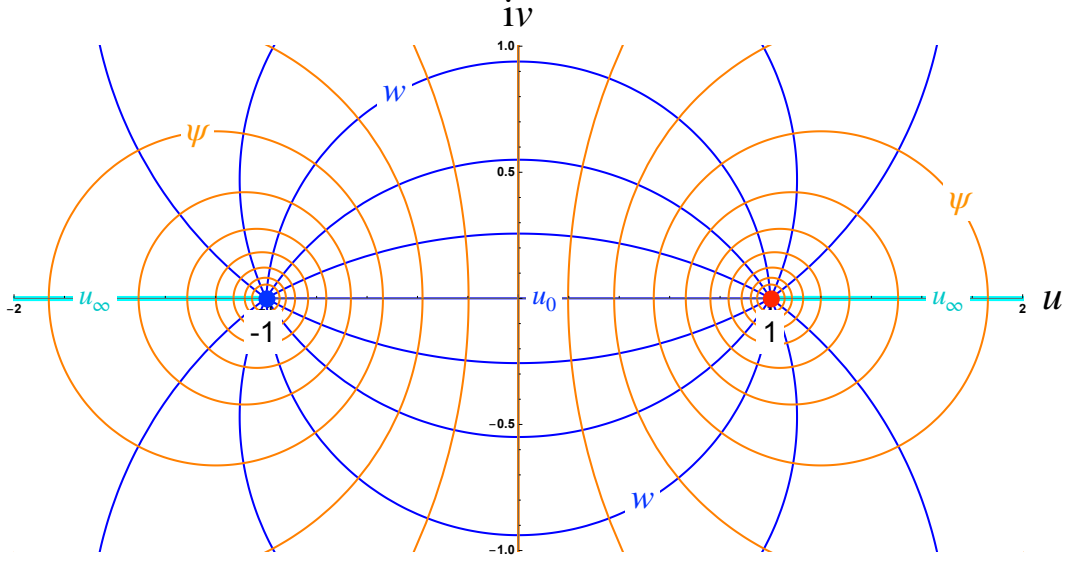


Figure 1.2: Phase portrait of complex ODEs (1.25) – (1.27) for the spatially homogeneous heteroclinic orbit $\Gamma : W_- \rightsquigarrow W_+$. Orbits $r \mapsto \Gamma(r + is) = u + iv$ of (1.27), (1.25), in real time r , are circular arcs (blue). They are heteroclinic from source $W_- = W_\infty = +1$ (red dot) to sink $W_+ = W_0 = -1$ (blue dot). The π -periodic orbits $s \mapsto \psi(s) = \Gamma(r - is) = u + iv$ of (1.26), in contrast, are full circles (orange), each with one of the two equilibria $W_\pm = \mp 1$ in the interior. Because the flows in real and imaginary time commute, the orange circles also serve as isochrones which globally synchronize the blue trajectories. Vice versa, the blue circle segments are isochrones which globally synchronize the orange periodic solutions. The imaginary v -axis (orange) blows up in finite time $s^* = \pm\pi/2$; see (1.29). On the Riemann sphere \mathbb{C}_∞ , this is just a longitude circle of period π through the poles 0 and ∞ . The real u -axis features the real heteroclinic orbit $u_0 : +1 \rightsquigarrow -1$, in blue, as well as the two cyan parts of the blow-up heteroclinic $u_\infty : +1 \rightsquigarrow \infty$ and the blow-down heteroclinic $u_\infty : \infty \rightsquigarrow -1$. On the Riemann sphere \mathbb{C}_∞ , these two segments combine to another longitude circle, perpendicular to the first at the polar intersections 0 and ∞ . In conclusion, the blue bounded heteroclinic orbit u_0 on the real u -axis, in real time, gives rise to finite time blow-up and blow-down on the orange imaginary v -axis, in imaginary time, when started at $u = v = 0$. The complex viewpoint also reveals blue real heteroclinicity u_0 and the cyan real blow-up / blow-down segments u_∞ as two aspects of one and the same underlying complex object Γ .

Without loss of generality, let us fix $\Gamma(0) = 0$. Explicitly, $v = 0$ in (1.27) then identifies the biholomorphic cylinder map (1.28) as

$$(1.30) \quad \Gamma(t) = -\tanh t,$$

first for real $t = r \in \mathbb{R}$, i.e. for $u_0 : 1 \rightsquigarrow -1$, and then for all $t \in \mathbb{C}$, by analytic continuation. This identifies $r_0 = 0$ and the blow-up solution

$$(1.31) \quad \psi(s) = -i \tan s.$$

Complex time shifts of Γ , in (1.28), induce the fractional linear, biholomorphic automorphisms of the Riemann sphere \mathbb{C}_∞ which fix ± 1 . In (1.30), this amounts to the elementary addition theorems for the hyperbolic tangent.

In passing, we note that the real and imaginary parts of the inverse function $\operatorname{arctanh}$ of the solution (1.30) are first integrals of (1.26) and (1.25), respectively. Specifically, the heteroclinic orbits of (1.27), (1.25), in real time $t = r$, foliate the cylinder $\mathbb{C}_\infty \setminus \{\pm 1\}$ into

segments of invariant Euclidean circles through $w = \pm 1$, with centers on the imaginary v -axis, blue and cyan in figure 1.2. The π -periodic orbits of (1.27), in the Schrödinger variant (1.26) of imaginary time $t = is$, define a perpendicular foliation into circles with centers $w = a \in \mathbb{R}$, $1 < |a| \leq \infty$ on the real u -axis, and radii $0 < \sqrt{a^2 - 1} \leq \infty$. The straight axes themselves have "centers at infinity", as already Cusanus has remarked [Ku1440].

Only in the spatially homogeneous cases (1.25), (1.26), of course, we can also trivialize the cylinder map (1.28), e.g. by the fractional linear, biholomorphic automorphism $w \mapsto (z + 1)/(z - 1)$ of the Riemann sphere \mathbb{C}_∞ . This maps the equilibria $W = \pm 1$ to ∞ and 0 , respectively. It also globally linearizes the quadratic complex ODE $\dot{w} = w^2 - 1$, alias (1.27), to become $\dot{z} = -2z$. In z , the heteroclinic orbits of (1.25) are inward radial, and the periodic orbits of (1.26) are circles of constant radius $|z|$. For general scalar ODEs $\dot{w} = g(w)$, we continue this discussion in section 7.3.

1.9 Outline

We proceed as follows. In section 2 we prove theorem 1.1. Section 3 adapts the classical approach of Weierstrass elliptic functions to derive the bifurcation diagram 1.1 of all real equilibria. In particular, lemma 3.1 summarizes known Fourier expansions which hold globally along the bifurcating branches W_n . In section 4, explicit eigenvalue expansions to second order, at the pitchfork bifurcations, then allow us to establish unstable spectral nonresonance for all but a discrete set of parameters λ . This proves theorem 1.2, for the quadratic heat equation (1.9). The proof of theorem 1.3 on fast unstable manifolds is deferred to section 5. Blow-up in the quadratic Schrödinger equation (1.16), contingent to heteroclinicity in the heat equation (1.9), is established in section 6. We conclude with a rather detailed discussion. See section 7.1 for a summary. Hurried readers interested in just some pertinent literature are encouraged to jump to section 7.5, directly and at their own risk.

1.10 Acknowledgment

This paper is dedicated to the memory of Marek Fila, a source of inspiration and generous friendliness for decades. He was the first to draw our attention to the topic of PDE blow-up, always most encouragingly and never losing faith in us, until we finally ventured to present this paper. We will miss his cheerful comments forever.

We are also indebted to Vassili Gelfreich, for very patient explanations of his profound work on exponential splitting asymptotics, to Anatoly Neishtadt for lucid conversations on adiabatic elimination, to Jonathan Jaquette and Jean-Philippe Lessard for generously sharing and discussing numerical details of [JLT22a, JLT22b], and to Karsten Matthies, Carlos Rocha, Jürgen Scheurle and late Claudia Wulff, for their lasting interest.

2 Real eternal contradicts complex entire

In this section we prove our main abstract result, theorem 1.1. We work in the setting of analytic semigroups Φ^t in sectors $t \in \mathfrak{S}_\Theta$ on a Banach space X , with $Y := X^\alpha$ and norm $\|\cdot\|$ on Y ; see section 1.2. Our proof is indirect: we will assume the heteroclinic orbit $\Gamma : W_- \rightsquigarrow W_+$ between hyperbolic equilibria W_\pm , in real time r , globally extends to a complex entire solution $\Gamma(t)$, $t = r + is \in \mathbb{C}$, of (1.1). See assumption (i).

Theorem 1.1, as well as its proof, is quite asymmetric with respect to the two equilibria W_\pm . One difficulty arises when parts of the heteroclinic orbits $r \mapsto \Gamma(r + is)$, in real time r and for fixed $s \neq 0$, traverse local neighborhoods of W_\pm multiple times, before settling into the limiting equilibrium W_+ . For sufficiently large $|s|$, potentially, this could happen in arbitrarily small neighborhoods. At W_+ , assumption (ii) excludes this difficulty by local asymptotic stability. At W_- , however, and in reverse time $r \rightarrow -\infty$, we cannot just assume this first difficulty away.

A second difficulty arises for estimates in the imaginary time direction is . Note the absence, in general, of a strongly continuous semigroup

$$(2.1) \quad s \mapsto \Phi^{is}$$

on all of Y , in imaginary time $t = is$. In particular, nonexistent Φ^{is} cannot commute with sectorial Φ^t , $t \in \mathfrak{S}_\Theta$, in the sense of (1.4). Restricted to the (supposedly) entire heteroclinic orbit $\Gamma(r + is)$, however, the semigroup acts as a flow on Γ , globally in forward, backward, and sideways time directions $t \in \mathbb{C}$, by time shift

$$(2.2) \quad \Phi^t \Gamma(t_0) := \Gamma(t + t_0).$$

Commutativity, continuity, and even analyticity of Φ^t now hold trivially, for all $t, t_0 \in \mathbb{C}$, under this restriction. Still, we are lacking boundedness estimates and recurrence properties, in imaginary time.

Spectral non-resonance assumption (iv) will come to our rescue. The significance lies in *Poincaré's theorem on analytic linearization*; see [IY08] for a complete proof. In absence of spectral resonances, the theorem provides a complex analytic, local near-identity diffeomorphism $\mathfrak{P} : (E_-^u, 0) \rightarrow (W_-^u, W_-)$ which linearizes the ODE flow within the local unstable manifold W_-^u , near the equilibrium W_- . Note the identical embedding $\mathfrak{P}'(0) : E_-^u \hookrightarrow Y$ of the finite-dimensional unstable eigenspace $E_-^u = T_{W_-} W_-^u$, in our case.

Restricted to the local unstable manifold W_-^u , all the way, let us now consider the diagonalizable linearization $L = A + f'(W_-)$ on E_-^u , with real and totally unstable spectrum, i.e. $\text{spec } L > 0$. In imaginary time $t = is$, that real spectrum is left rotated to become purely imaginary. Therefore oscillations remain small, i.e. within the region of validity of the linearization, uniformly for all imaginary parts $s \in \mathbb{R}$. Specifically, in the notation of (1.8), we observe

$$(2.3) \quad \Gamma(t) = \mathfrak{P} \left(\sum_{0 \leq j < i(W_-)} a_j \exp(\mu_j t) \varphi_j \right)$$

for all $r = \operatorname{Re} t \leq 0$ and suitable coefficients $a_j \in \mathbb{C}$, provided $\|\Gamma(0) - W_-\| < \varepsilon$ is chosen small enough. Indeed, the coefficients $a_j \exp(\mu_j t)$ of any eigenvector φ_j remain unchanged, in absolute value, under the analytically equivalent linearized flow in imaginary time $t = is$.

Moreover, any solution $w(is)$ starting at w_0 near W_- is quasi-periodic in imaginary time s . See [Bo32, Bes32, Har85, Fie23] for details on almost- and quasi-periodicity. In particular, w_0 is *Poisson stable* in, both, forward and backward imaginary time $t = is$, i.e.

$$(2.4) \quad w_0 \in \alpha_{\mathbb{R}}(w_0) \cap \omega_{\mathbb{R}}(w_0).$$

Here the sets of accumulation points of global solutions $w(\pm t_n)$ are called the ω - and the α -limit set $\omega_{\mathbb{R}}(w_0)$ and $\alpha_{\mathbb{R}}(w_0)$, respectively, for real times $t_n = r_n \nearrow +\infty$. Real-time heteroclinic orbits $\Gamma : W_- \rightsquigarrow W_+$, for example, are characterized by $\alpha_{\mathbb{R}}(\Gamma_0) = \{W_-\}$ and $\omega_{\mathbb{R}}(\Gamma_0) = \{W_+\}$. For imaginary times $t_n = is_n$ and $s_n \nearrow +\infty$, we denote the corresponding limit sets by $\omega_{\mathbb{R}}(w_0)$ and $\alpha_{\mathbb{R}}(w_0)$.

Non-resonant Poincaré linearization, quasi-periodicity, and Poisson stability apply, in particular, within the complex analytic local unstable manifold $w_0 := \Gamma_0 \in W_-^u$ of the hyperbolic heteroclinic source W_- .

Proof of theorem 1.1.

Assumptions (i), (iii), and (iv) allow us to fix

$$(2.5) \quad w_0 = \Gamma_0 = \Gamma(0) \in W_-^u$$

close enough to W_- in the local unstable manifold W_-^u , such that Poisson stability (2.4) holds. Let $C := \sup \|\Gamma(\mathbb{R})\|$. Inductively, we will establish rectangle boundaries $0 \leq r_n, s_n \nearrow +\infty$ on which Γ is bounded by $C + 1$, i.e.

$$(2.6) \quad |r| = r_n, |s| \leq s_n \quad \Rightarrow \quad \|\Gamma(r + is)\| \leq C + 1,$$

$$(2.7) \quad |r| \leq r_n, |s| = s_n \quad \Rightarrow \quad \|\Gamma(r + is)\| \leq C + 1.$$

Since complex entire $\Gamma(t) \in \mathbb{C}$ is assumed to be complex differentiable in $t = r + is \in \mathbb{C}$, the harmonic maximum principle establishes the same uniform bound $C + 1$ in the interior of any rectangle, and hence for all $\Gamma(\mathbb{C})$. By Liouville's theorem, Γ must then be constant. This contradicts our definition of heteroclinicity, and will complete the proof.

To establish sequences $r_n, s_n \nearrow \infty$ of rectangle boundaries, where the bounds $\|\Gamma\| \leq C + 1$ of (2.6), (2.7) hold, we only consider imaginary parts $s \geq 0$; the case $s \leq 0$ is analogous. However, the case $0 \leq r \leq r_n \nearrow +\infty$ of forward convergence to the locally asymptotically stable equilibrium W_+ , and the case $0 \geq r \geq -r_n \searrow -\infty$ of convergence to the nonresonantly unstable equilibrium W_- , in backward time, are quite different.

Step 1: $0 \geq r \geq -r_n \searrow -\infty$.

Our unstable spectral non-resonance assumption (iv) and Poincaré linearization (2.3) allow us to pick $\Gamma_0 = \Gamma(0)$ within the domain of Poincaré linearization (2.3) in the *local*

unstable manifold W_-^u of the unstable source equilibrium W_- of $\Gamma : W_- \rightsquigarrow W_+$. In particular, we may assume

$$(2.8) \quad \|\Gamma(r + is) - W_-\| < 1$$

for all $r \leq 0$, in the first place.

This settles estimates (2.6), (2.7) in the case $0 \geq r \geq -r_n \searrow -\infty$ of backward time.

Step 2: $0 \leq r \leq r_n \nearrow +\infty$.

We start from a few elementary observations concerning asymptotic stability of equilibria W . By standard definition of local asymptotic stability in real time, there exists $0 < \varepsilon < 1$ such that the following two statements hold for $w(t) = \Phi^t(w_0)$, $0 \leq t = r \in \mathbb{R}$:

$$(2.9) \quad \|w_0 - W\| < \varepsilon \quad \Rightarrow \quad \|w(r) - W\| < 1,$$

$$(2.10) \quad \|w_0 - W\| < \varepsilon \quad \Rightarrow \quad \lim_{r \rightarrow \infty} w(r) = W.$$

Since linear asymptotic stability implies nonlinear local asymptotic stability, assumption (ii) of theorem 1.1 implies that these statements hold true for $W := W_+$, in our heteroclinic setting. Decreasing the sectorial angle $\Theta > 0$, if necessary, we reach the same conclusions for the complex sector $t \in \mathfrak{S}_\Theta$.

Starting our induction at $r_1 = s_1 = 0$, there is nothing to prove. We assume r_{n-1}, s_{n-1} have been chosen, and we construct $r_n \geq r_{n-1} + 1$, $s_n \geq s_{n-1} + 1$ next.

For the complex entire heteroclinic orbit $\Gamma : W_- \rightsquigarrow W_+$, we first observe

$$(2.11) \quad \lim_{r \rightarrow \infty} \Gamma(t_0 + r) = W_+$$

for real r and all $t_0 \in \mathbb{C}$. This follows from (2.10), strong continuity, and because the semigroups commute in the sector \mathfrak{S}_Θ ; see (1.4).

Consider any $w_0 = \Gamma(t_0) \in \Gamma(\mathbb{C})$. Then the following statements hold for all $\tilde{w}_0 \in Y$:

$$(2.12) \quad \forall w_0 \exists r_0 > 0 : \quad r \geq r_0 \Rightarrow \|w(r) - W_+\| < \varepsilon;$$

$$(2.13) \quad \forall w_0, r_0, \varepsilon' > 0 \exists \delta > 0 : \|\tilde{w}_0 - w_0\| < \delta, 0 \leq r \leq r_0 \Rightarrow \|\tilde{w}(r) - w(r)\| < \varepsilon';$$

$$(2.14) \quad \forall w_0 \exists r_0, \delta > 0 : \|\tilde{w}_0 - w_0\| < \delta \quad \Rightarrow \quad \|\tilde{w}(r_0) - W_+\| < \varepsilon;$$

$$(2.15) \quad \forall w_0 \exists r_0, \delta > 0 : \|\tilde{w}_0 - w_0\| < \delta, \quad r \geq r_0 \Rightarrow \|\tilde{w}(r) - W_+\| < 1.$$

Indeed, convergence (2.11) implies (2.12). Strong continuity on compact time intervals implies (2.13). Together, (2.12) with $r := r_0$, and (2.13) with $\varepsilon' := \varepsilon - \|w(r_0) - W_+\| > 0$, imply (2.14).

Combining (2.14) with (2.9) proves (2.15). Only this last step uses local asymptotic stability property (2.9) of W_+ . Specifically, w_0 in (2.9) is chosen as $\tilde{w}(r_0)$ from (2.14).¹

¹For unstable targets W_+ , this step (2.15) fails: although $\tilde{w}(r_0)$ would be an element of the *global* stable manifold W_+^s of the hyperbolic unstable equilibrium W_+ , near W_+ , it might fail to lie in the *local* stable manifold W_+^s . The local stability estimate (2.9), however, only applies in the *local* stable manifold W_+^s of hyperbolic equilibria W_+ . In step 1, i.e. near W_- , unstable spectral non-resonance and Poincaré linearization have circumnavigated this difficulty.

To establish the required estimate (2.7) at a suitable top boundary $s = s_n$, we recall our choice of $\Gamma_0 = \Gamma(0)$, in step 1, such that Poisson stability (2.4) holds for $w_0 = \Gamma_0$, in imaginary time. Pick r_0 and δ according to (2.15), for $w_0 := \Gamma_0$. Reduce δ , if necessary, such that (2.13) holds, in addition, for $w_0 := \Gamma_0$ and $\varepsilon' := 1$. Then

$$(2.16) \quad \exists \delta > 0 : \quad r \geq 0, \quad \|\tilde{w}_0 - \Gamma_0\| < \delta \quad \Rightarrow \quad \|\tilde{w}(r)\| \leq C + 1.$$

Since $w_0 = \Gamma_0 \in \omega_{\mathbb{R}}(\Gamma_0)$ by (2.4), we may choose $s_n \geq s_{n-1} + 1$ such that $\tilde{w}_0 := \Gamma(is_n)$ satisfies $\|\tilde{w}_0 - \Gamma_0\| < \delta$, in (2.16). This proves claim (2.7), at the top boundary, independently of any choice for the right boundary r_n .

To construct $r_n \geq r_{n-1} + 1$, we can now cover the compact set $\Gamma(i[0, s_n])$ by a finite collection of $\delta = \delta_j$ neighborhoods of $w_0 = w_j$, with associated $r = r_{0j}$, such that (2.15) holds for all j . Letting r_n also exceed the maximal r_{0j} then, (2.16) establishes the claimed right boundary estimate (2.6). This settles the case $0 \leq r \leq r_n \nearrow +\infty$ of forward time, and completes the proof of theorem 1.1. \bowtie

We recall how our proof of corollary 1.5 has circumvented the difficulty mentioned in the footnote concerning (2.15). In the fastest unstable manifold of W_- , of dimension $d = 1$, any entire $\Gamma(r + is)$ has to be periodic in s of minimal period $p = 2\pi/\mu_0$; see (1.19) in section 1.7. Therefore local stability (2.9) was replaced by strong continuity, in the bounded period interval $0 \leq s \leq p$. This mends the gap and proves theorem 1.1, as before.

In the ODE case $X = \mathbb{C}^N$ of [Fie23], Poincaré linearization and quasi-periodicity at, both, W_-^u and W_+^s , came to rescue. In fact, the proof there was based on Cauchy's theorem, to compare the conflicting Fourier-coefficients with respect to s , at fixed r near $\pm\infty$. This was possible even though the heteroclinic orbit $\Gamma(r + is)$ might lose quasi-periodicity in s , at intermediate r .

3 The quadratic heat equation: Weierstrass equilibria

As announced in section 1.4, we now embark on our study of the quadratic heat equation (1.9). Specifically, we address spatially non-homogeneous real equilibria W , i.e. non-constant solutions $W(x)$ of the Neumann ODE boundary value problem

$$(3.1) \quad W_{xx} + 6W^2 - \lambda = 0, \quad \text{for } 0 < x < \frac{1}{2},$$

$$(3.2) \quad W_x = 0, \quad \text{for } x = 0, \frac{1}{2};$$

see (1.11). Neumann boundary conditions (3.2), and our focus on real heteroclinic PDE orbits $\Gamma : W_- \rightsquigarrow W_+$ between real equilibria $W = W_{\pm}$, require a few adaptations of the standard complex results. We harmonize the bifurcation viewpoint of figure 1.1 with classical Fourier-expansions of the Weierstrass function \wp , for modular parameters $\tau \rightarrow i\infty$. Throughout we refer to [Akh90, Fri1916, Lan87, Lam09] for details in complex analysis language.

For $m, n \in \mathbb{Z}$ and $\text{Im } \tau > 0$, let $\omega = m + n\tau$ denote the elements of the integer lattice $\Lambda := \langle 1, \tau \rangle_{\mathbb{Z}}$, with $\Lambda' := \Lambda \setminus \{0\}$. Then the associated Weierstrass function $\wp = \wp(\tau; z)$ is defined by the infinite partial fraction

$$(3.3) \quad \wp(\tau; z) := z^{-2} + \sum_{\omega \in \Lambda'} ((z - \omega)^{-2} - \omega^{-2}).$$

Note how \wp is meromorphic of degree -2 , and doubly periodic in z with lattice periods $1, \tau$. By Liouville's theorem, $\wp = \wp(z)$ satisfies the ODE

$$(3.4) \quad \wp_z^2 = 4\wp^3 - g_2\wp - g_3, \quad \text{for } z \in \mathbb{C} \setminus \Lambda, \text{ with coefficients}$$

$$(3.5) \quad g_2 = 60 \sum_{\omega \in \Lambda'} \omega^{-4},$$

$$(3.6) \quad g_3 = 140 \sum_{\omega \in \Lambda'} \omega^{-6}.$$

Standard calculus of residues on \wp_z locates the three zeros ω_j of \wp_z , and hence the zeros $e_j = \wp(\omega_j)$ of the cubic polynomial $4\xi^3 - g_2\xi - g_3$, at the half-periods ω_j of $z \mapsto \wp(z)$:

$$(3.7) \quad \omega_1 = \frac{1}{2}, \quad \omega_2 = \frac{\tau}{2}, \quad \omega_3 = \frac{1}{2} + \frac{\tau}{2}.$$

3.1 Lemma. *Any spatially non-homogeneous real solution W of the Neumann ODE boundary value problem (3.1), (3.2) takes the form $W = W_n$ at $\lambda = \lambda_n$, where*

$$(3.8) \quad \lambda_n = \frac{1}{2}n^4 g_2, \quad \text{and either}$$

$$(3.9) \quad W_n(x) = -n^2 \wp(\omega_2 + nx), \quad \text{or}$$

$$(3.10) \quad W_n(x) = -n^2 \wp(\omega_3 + nx),$$

for some purely imaginary modular parameter $\tau = i\vartheta$, $\vartheta > 0$ and $n = 1, 2, 3, \dots$

An explicit Fourier expansion in terms of real $h = \pm \exp(-\pi\vartheta)$ reads

$$(3.11) \quad \lambda_n = \frac{2}{3}(n\pi)^4 \left(1 + 240 \sum_{k \geq 1} \sigma_3(k) h^{2k}\right),$$

$$(3.12) \quad W_n(x) = (n\pi)^2 \left(\eta + 8 \sum_{k \geq 1} k \frac{h^k}{1 - h^{2k}} c_{nk}\right), \quad \text{where}$$

$$(3.13) \quad \eta = \frac{1}{3} - 8 \sum_{k \geq 1} k \frac{h^{2k}}{1 - h^{2k}}.$$

Here $\sigma_3(k)$ in (3.11) abbreviates the sum of the third powers of all divisors of k , including 1 and k itself. In (3.12), the spatial Fourier terms $\cos(2\pi n k x)$ are abbreviated by c_{nk} .

As in figure 1.1, note the supercritical pitchfork bifurcations from the spatially homogeneous solution $h = 0$, alias $\tau = i\infty$, $\vartheta = +\infty$, at

$$(3.14) \quad \lambda_{n0} = \frac{2}{3}(n\pi)^4, \quad W_{n0}(x) \equiv \frac{1}{3}(n\pi)^2 = \sqrt{\lambda_{n0}/6} = W_{\infty}.$$

Proof. We consider complex solutions $W = W(x)$, $x \in \mathbb{R}$ of the Neumann boundary value problem (3.1), (3.2) first. Spatially homogeneous solutions are obtained, trivially, as the square roots of $\lambda/6$. Suppose therefore that W is non-constant in x . By integration of the Hamiltonian pendulum (3.1) with respect to x , we obtain the conservation

$$(3.15) \quad W_x^2 = -4W^3 + 2\lambda W + 2E,$$

of some complex “energy” parameter $E \in \mathbb{C}$. Reflection through the Neumann boundary conditions (3.2), and reversibility of the second order equation with respect to $x \mapsto -x$ shows that $W = W(x)$ must possess (not necessarily minimal) period 1 in x . Let $1/n$ denote the minimal period of $x \mapsto W(x)$, and define

$$(3.16) \quad \tilde{\wp}(x) := -n^{-2}W(x/n).$$

Then $\tilde{\wp}(x)$ possesses minimal period 1 in x , and solves (3.4) with

$$(3.17) \quad g_2 = 2n^{-4}\lambda \quad \text{and} \quad g_3 = -2n^{-6}E.$$

Since $W(x)$ is neither constant, nor homoclinic, the discriminant $\Delta := g_2^3 - 27g_3^2$ of the cubic polynomial $4\xi^3 - g_2\xi - g_3$ is nonzero. In particular,

$$(3.18) \quad \tilde{\wp}(x) = \wp(z_0 + x)$$

coincides with the standard Weierstrass function, for a suitable integer lattice Λ and up to a time-shift $z_0 \in \mathbb{C}$. The modular parameter τ is determined uniquely from g_2, g_3 in (3.17), up to an $SL_2(\mathbb{Z})/\{\pm \text{id}\}$ fractional linear transformation of τ , via Klein’s modular invariant $J = g_2^3/\Delta$.

The Neumann boundary conditions (3.2) and reversibility in x , finally, determine boundary values $\tilde{\wp}(x) \in \{e_1, e_2, e_3\}$ at $x = 0, 1/2$. Only from here on, we use that the parameter $\lambda > 0$ and the solutions W are assumed to be real. We will discuss complex solutions in section 7.5; in particular see (7.23). In view of (3.7), real W imply $z_0 = \omega_2$ or $z_0 = \omega_3$. Indeed, the choice $z_0 = \omega_1$ would lead to singular solutions $\tilde{\wp}(x)$ and $W_n(x)$. Non-horizontal evaluations of \wp would lead to non-real complex solutions; see (7.23). This proves the alternative claims of (3.9) and (3.10), respectively, and (3.8), in either case.

We now address the case (3.9), where $\tilde{\wp}(x) = \wp(\omega_2 + x)$ tracks the 1-periodically rescaled version $-n^{-2}W(x/n)$ between e_2 and e_3 , for $0 < x < 1/2$; see (3.16) and (3.7). Standard Fourier expansions of \wp and g_2 in terms of

$$(3.19) \quad h = \exp(\pi i \tau)$$

then prove claims (3.12), (3.13), and (3.11), via the scaling (3.16). Note absolute convergence of the sums: $\text{Im } \tau > 0$ implies $0 < |h| < 1$. Similar expansions have been derived in [Fri1916], section I.4.9, (14)–(16), and, skipping g_2 , in [Akh90], Table X, p. 204. In different notation, see [Lan87], section 4.2, and for g_2 , but not \wp , also [Apo90], Theorem 1.18 in section 1.14. The notationally confusing, but elementary, arithmetic details to derive the specific versions (3.11)–(3.13) from any of these references are left to the diligent reader.

We assume real solutions W_n , from now on. We will address case (3.10) after first identifying the modular parameter τ . The Fourier expansion (3.12) in terms of c_{nk} has to be real now, for all $0 < x < 1/2$. In particular all coefficients must be real. For $k = 1$ and nonzero complex h , this implies that there exists $a \in \mathbb{R}$ such that

$$(3.20) \quad h/(1 - h^2) = 1/a.$$

The solutions $h = \frac{1}{2}(-a \pm \sqrt{a^2 + 4})$ of the resulting quadratic equation for h are therefore real, too. By (3.19) and $0 < |h| < 1$, this implies the alternative

$$(3.21) \quad 0 < h = +\exp(-\pi\vartheta) < 1, \quad \tau = i\vartheta, \quad \text{or}$$

$$(3.22) \quad -1 < h = -\exp(-\pi\vartheta) < 0, \quad \tau = i\vartheta + 1,$$

for modular parameters τ in the upper half plane $\text{Im } \tau > 0$, and for $\text{Re } \tau$ taken mod 2. Here $0 < \vartheta < \infty$. Comparing the cases $\tau = i\vartheta$ and $\tau = i\vartheta + 1$ we see how the roles of ω_2 and ω_3 in (3.7) interchange. Since (3.12) follows from (3.9), for the first case (3.21) and $0 < h < 1$, this also proves the same Fourier expansion (3.12) by (3.10), in the second case (3.22) and for $-1 < h < 0$.

Note how the two cases $\pm h > 0$ correspond to the upper (orange) and lower (blue) branches of the pitchfork bifurcations in figure 1.1. Also $\lambda_n \geq \lambda_{n0}$ increases strictly with h , globally from the bifurcation point (3.14) at $h = 0$, alias $\tau = i\infty$, $\vartheta = +\infty$ in (3.11)–(3.13).

This proves the lemma. ∞

For real solutions W_n , the parameter $E \in \mathbb{R}$ is the classical pendulum energy. Note positive discriminant $\Delta > 0$, since W_n possesses two real extrema: e_2 and e_3 . In particular $g_2^3 = \Delta + 27g_3^2 > 0$, and hence $\lambda > 0$ by (3.17). More precisely, $\lambda > \lambda_{10} = \frac{2}{3}\pi^4$, by (3.11), (3.14).

The appearance of the modular parameter $\tau \bmod 2$ in (3.21), (3.22) might surprise some experts (and non-experts, like the authors) who would properly have expected $\tau \bmod 1$, from biholomorphic equivalence of complex tori \mathbb{C}/Λ . The discrepancy is caused by our selection of Neumann boundary conditions, which distinguish between boundary values $-n^2e_2$ and $-n^2e_3$ of $W_n(x)$ appearing on the left boundary $x = 0$, and thus distinguish between upper and lower branches $h > 0$ and $h < 0$ in figure 1.1.

The same procedure which has identified all real solutions of the ODE boundary value problem (3.1), (3.2), in lemma 3.1, can easily be modified to also identify all remaining complex solution *branches*. Indeed, to encounter an interval of branch parameters λ , rather than just a totally disconnected set of singletons, we have to work with modular parameters h such that λ remains real, on at least an interval of h . Therefore $h^2 = \exp(2\pi i\tau)$ must remain real, in the complex Fourier expansion (3.11) of $\lambda = \frac{1}{2}n^4g_2$; see (3.17). In other words, $\tau = \frac{1}{2} + i\vartheta$, with real part mod 1. This parametrizes the remaining two complex branches which bifurcate subcritically at the same bifurcation points (3.14), for purely imaginary h .

Our present PDE techniques do not allow us to determine global heteroclinic orbits among complex branches, in real or complex time. See the discussion section 7.5 for further comments and examples, particularly on the purely quadratic “vertical” case of the singleton $\lambda = 0$. There, our branch argument fails due to complex rescaling (7.23).

4 The quadratic heat equation: non-resonance at bifurcation

We continue our study of the quadratic heat equation (1.9) with Fourier expansions of eigenfunctions and eigenvalues, up to order h^2 in the Fourier term $h = \exp(\pi i \tau)$ of the modular parameter $\tau \rightarrow i\infty$. Our starting point is lemma 3.1 on the real equilibrium branches (λ_n, W_n) parametrized over real h . In particular we prove theorem 1.2 on unstable spectral non-resonance at equilibria $W_- = W_n$, for $1 \leq n \leq 22$. In view of theorem 1.1, proved in section 2, it only remains to exclude unstable spectral resonances (1.8), according to assumption 1.1(iv).

Proof of theorem 1.2.

The spectrum of the linearization $L = A + f'(W)$ at $W = W_n$ or $W = W_\infty$ is given by the Sturm-Liouville eigenvalues $\mu = \mu_k$ and eigenfunctions $\varphi = \varphi_k$ of the Neumann boundary value problem

$$(4.1) \quad \mu \varphi = \varphi_{xx} + 12W\varphi, \quad \text{for } 0 < x < 1/2,$$

$$(4.2) \quad 0 = \varphi_x, \quad \text{for } x = 0, 1/2.$$

See (1.12). We suppress the subscripts k and n , for the moment.

Case 1: $W_- = W_\infty$

The case $W = W_\infty = \sqrt{\lambda/6}$ is explicit. The unstable spectrum at any $\lambda > 0$ is given by

$$(4.3) \quad 0 < \mu = \mu_{\infty k} = 2\sqrt{6\lambda} - (2\pi k)^2, \quad \text{for } 0 \leq k^2 < \pi^{-2}\sqrt{\frac{3}{2}}\lambda,$$

with eigenfunctions $c_k(x) = \cos(2\pi kx)$. The resonance condition (1.8) reads

$$(4.4) \quad (|\mathbf{m}| - 1)\pi^{-2}\sqrt{\frac{3}{2}}\lambda = -j^2 + \sum_k m_k k^2 \leq |\mathbf{m}| \bar{k}^2.$$

Here $m_k \geq 0$, and \bar{k} denotes the maximal k such that $m_k > 0$. As long as $\bar{k}^2 < \pi^{-2}\sqrt{\frac{3}{2}}\lambda$ stays away from its upper bound, we obtain upper bounds on $|\mathbf{m}|$, and hence discrete sets of resonant λ . The limiting cases $\pi^{-2}\sqrt{\frac{3}{2}}\lambda \searrow k^2 = n^2$ of vanishing eigenvalue $\mu_{\infty n} = 0$, on the other hand, precisely identify the points $\lambda = \lambda_{n0}$ of pitchfork bifurcations; see (3.14) and (1.14).

This establishes the result of theorem 1.2, for the case $W_- = W_\infty$.

In fact, it is easy to construct examples of resonant parameters accumulating to the bifurcation points. Integer $m \nearrow \infty$, for example, provide a sequence of 1: m resonances

$\mu_{\infty 0} = m\mu_{\infty n}$ in the sense of (1.8). Resonance occurs at parameters $\lambda = \lambda'_m \searrow \lambda_{n0}$ defined by the second equality in

$$(4.5) \quad \mu_{\infty 0} = 2\sqrt{6\lambda'_m} = m(2\sqrt{6\lambda'_m} - (2\pi n)^2) = m\mu_{\infty n}.$$

Case 2: $W_- = W_n$

Since all eigenvalues are algebraically simple and the equilibrium $W = W_n$ depends analytically on h , so do the eigenvalues μ and properly normalized eigenfunctions φ . Suppressing standing subscripts n, k of W, μ, φ , all the way, we can therefore expand at the bifurcation point $h = 0$ and write

$$(4.6) \quad W = (n\pi)^2(W_0 + W_1h + W_2h^2 + \dots),$$

$$(4.7) \quad \mu = 4\pi^2(\mu_0 + \mu_1h + \mu_2h^2 + \dots),$$

$$(4.8) \quad \varphi = \varphi_0 + \varphi_1h + \dots,$$

with new indices $0, 1, 2$ indicating h -expansions. In view of lemma 3.1, and (3.12) in particular, we cover both bifurcating pitchfork branches (3.9) and (3.10) by $0 < \pm h < 1$.

Truncating the expansions (3.12), (3.13), we obtain

$$(4.9) \quad W_0 = \frac{1}{3},$$

$$(4.10) \quad W_1 = 8c_n,$$

$$(4.11) \quad W_2 = -8 + 16c_{2n}.$$

We now insert the h -expansions (4.6)–(4.8) into the spectral linearization (4.1), (4.2) and compare coefficients. At level h^0 we get

$$(4.12) \quad \mu_0 = n^2 - k^2, \quad \varphi_0 = c_k.$$

Note how our choice $\varphi_0 = c_k$ scales the whole eigenfunction expansion. I.e., the Fourier term $c_k \in \ker(\mu_0 - \partial_{xx} - 6W_\infty)$ will be assumed absent in φ_1, \dots . At level h^1 , consequently, we have to distinguish the special case $k = n/2$, for even n :

$$(4.13) \quad \mu_1 = 0, \quad \varphi_1 = 12n\left(\frac{1}{n-2k}c_{n-k} + \frac{1}{n+2k}c_{n+k}\right), \quad \text{for } k \neq n/2,$$

$$(4.14) \quad \mu_1 = 12n^2, \quad \varphi_1 = 6c_{3n/2}, \quad \text{for } k = n/2.$$

At level h^2 , we again have to distinguish the special case $k = n/2$. Since our main objective here is the eigenvalue coefficient $\mu_2\varphi_0$, scalar L^2 -multiplication of (4.1) by φ_0 eliminates the eigenfunction term φ_2 . We obtain

$$(4.15) \quad \mu_2 = 24n^2 \cdot \frac{11n^2 + 4k^2}{n^2 - 4k^2}, \quad \text{for } k \neq n/2,$$

$$(4.16) \quad \mu_2 = 48n^2, \quad \text{for } k = n/2.$$

Any linear resonance conditions (1.8), as well as the eigenvalues μ_j, μ_k themselves, are analytic in h . Therefore, any unstable resonance either holds identically in h , or at most at a discrete set of h , and hence of parameters λ by expansion (3.11). Since the pitchfork

bifurcations are supercritical, we can extend this argument to include the bifurcation points $\lambda = \lambda_{n0}$ themselves, this time. Indeed, the stable eigenvalue $\mu_n \nearrow 0$, for $\lambda \searrow \lambda_{n0}$, does not contribute to unstable resonance, this time.

We have to exclude identical resonance. In other words, it is sufficient to exclude resonances (1.8), separately, for each set of expansion coefficients μ_0, μ_1, μ_2 , and with the same integer vector \mathbf{m} . Computer checking of the resulting three explicit linear Diophantine conditions for \mathbf{m} excluded identical resonance, for $n \leq 22$.

This completes the proof of theorem 1.2. \boxtimes

5 The quadratic heat equation: fast unstable manifolds

We continue our study of the quadratic heat equation (3.1) with Neumann boundary (3.2). We address non-entire heteroclinic orbits $\Gamma : W_- \rightsquigarrow W_+$ which originate in the local d -dimensional fast unstable manifold W_-^{uu} of W_- . See section 1.5. The hyperbolic equilibrium $W = W_-$ can be homogeneous, i.e. $W = W_\infty$, or non-homogeneous, i.e. $W = W_n$. In either case, we consider dimensions $1 \leq d < n := i(W)$. In particular, we prove theorem 1.3 on unstable spectral non-resonance, for $d < 1 + \frac{1}{\sqrt{2}}n$; see (1.15).

Because the Sturm-Liouville spectrum at W consists of algebraically simple eigenvalues, the local d -dimensional fast unstable manifold W^{uu} always exists, characterized by exponential decay rates, in backward time, which exceed the eigenvalue $\mu_d > 0$; see (1.12) and (4.1), (4.2). The standard Perron proof for W^u in [Hen81], adapted for decay rates by exponentially weighted spaces, establishes local analyticity of W^{uu} .

Proof of theorem 1.3.

Our proof follows the lines of section 4, replacing the bound on $n = i(W)$ by a bound on $d/n < 1$. Our treatment is identical for the cases $W = W_n$ and $W = W_\infty$, because our assumption $d < n = i(W)$ eliminates the small positive eigenvalue $\mu_{\infty n}$ generated, supercritically, along the primary branch W_∞ at pitchfork bifurcation $\lambda \searrow \lambda_{n0}$. See section 4, case 1.

In fact we just show absence of identical resonances at order h^0 , in (4.6)–(4.8). By (4.12), that resonance condition can be estimated by

$$(5.1) \quad n^2 \geq n^2 - j^2 = \sum_{k=0}^{d-1} m_k (n^2 - k^2) \geq |\mathbf{m}| (n^2 - (d-1)^2),$$

for any choice of nonnegative integers m_k of order $|\mathbf{m}| \geq 2$. This implies

$$(5.2) \quad d \geq 1 + \frac{1}{\sqrt{2}}n,$$

i.e. the opposite of assumption (1.15). By contraposition, (1.15) prohibits identical unstable resonances and proves theorem 1.3. \boxtimes

As announced in section 1.5, we now indicate asymptotic optimality of the bound (1.15) for nonresonance at level h^0 . Choosing $j = 0$ and $|\mathbf{m}| = (0, \dots, 1, 1) \in \mathbb{N}_0^d$, we just have to solve resonance condition (1.8) for Pythagorean triples

$$(5.3) \quad (d-2)^2 + (d-1)^2 = n^2.$$

Explicit solutions are given by the successive co-prime convergents a/b of the 1-periodic continued fraction

$$(5.4) \quad 1 + \sqrt{2} = [2; 2, 2, 2, \dots],$$

related by a linear recursion of Fibonacci type. Indeed we may choose $n = a^2 + b^2$ and $\{d-2, d-1\} = \{a^2 - b^2, 2ab\}$ to achieve $\lim n/d = \sqrt{2}$. An explicit optimal example satisfying (5.2) is $n = 29$, $d = 22$.

6 The quadratic Schrödinger equation: blow-up and blow-down

Following up on section 1.6, we prove theorem 1.4 on blow-up $0 < s \nearrow s^*$ (and symmetric blow-down $0 > s \searrow -s^*$) in the complex Schrödinger equation (1.16). Blow-up will be shown to occur for certain initial conditions $\psi_0 := \Gamma(r_0)$ on eternal real heteroclinic solutions $\Gamma : W_- \rightsquigarrow W_0$ of the quadratic heat equation (1.9). We assume the equilibrium W_- is nonresonant, and Γ emanates from the unstable or strong unstable manifold of W_- under the assumptions of theorems 1.2 or 1.3, respectively.

Our construction of Schrödinger blow-up for $s \mapsto \psi(s) = \Gamma(r_0 + is)$, at imaginary time $0 < s = s^* < \infty$, will be based on blow-up of $r \mapsto w(r) := \Gamma(r + is_0)$ for the heat equation, at real time $r \nearrow r^*(s_0) < \infty$. Here r carries sectorial analyticity, whereas s only knows strong continuity. We then seek Schrödinger blow-up at $s^* = s_0$, for $r_0 := r^*(s_0)$.

Starting from just any $s_0 > 0$ such that $r^*(s_0) < \infty$, however, may run into trouble. In fact, the real heat semiflow Φ^r and the imaginary Schrödinger semiflow $S^s = \Phi^{is}$ may fail to commute, up to $r = r_0$, $s = s_0$, when other singularities of Γ to the lower left eclipse access to from $r + is = 0$ to $r_0 + is_0$. See the condition for commutativity (1.4).

In (6.2), our proof of theorem 1.4 will avoid this obstacle to commutativity, by the construction (6.1) of a left-infinite rectangle $\mathcal{R} \subset \mathbb{C}$ carrying analyticity of Γ , except at the upper right corner $r_0 + is_0$ where heat *and* Schrödinger blow-up will occur.

Proof of theorem 1.4.

By theorems 1.2 and 1.3, Γ cannot be complex entire. Therefore, real-time blow-up (1.5) of $r \mapsto \Phi^{r+is}(\Gamma_0) = \Gamma(r + is)$ has to occur, for some fixed $s = \hat{s} > 0$ and at some finite real time $r \nearrow r^*(\hat{s}) < \infty$. Here we have used reversibility (1.18) to restrict to $\hat{s} > 0$ and blow-up, rather than $\hat{s} < 0$ and blow-down, without loss of generality. We recall here, and will peruse, that due to nonresonance at W_- the heteroclinic solutions $\Gamma(r + is)$ emanating from W_- via W_-^u or W_-^{uu} are complex analytic and remain local, for all $r \leq 0$; see (2.8).

As in (1.20), let $-\infty < r < r^*(s) \leq \infty$ denote the maximal interval of existence of the solution $r \mapsto \Gamma(r + is) = \Phi^r(\Gamma(is))$, in real time r . Note complex analyticity of $\Gamma(t)$ in

the region $t \in \mathcal{D} := \{r + is \mid -\infty < r < r^*(s)\}$. By strong continuity of the sectorial semigroup Φ^t , the domain \mathcal{D} is open and, equivalently, $s \mapsto r^*(s)$ is lower semicontinuous. To reach a contradiction, as announced above, we will construct a left-infinite rectangle

$$(6.1) \quad \mathcal{R} := \{r + is \mid -\infty < r \leq r_0 < \infty, 0 \leq s \leq s_0 < \infty\} \subset \mathcal{D} \cup \{r_0 + is_0\},$$

such that only the upper right corner $r_0 + is_0$ is in the boundary $\partial\mathcal{D}$. For the special case of fastest heteroclinic orbits Γ , see also section 1.7.

The significance of the rectangle \mathcal{R} is that the real heat semigroup $r \mapsto \Phi^r$ and the imaginary Schrödinger flow $s \mapsto S^s = \Phi^{is}$ commute on $\Gamma_0 = \Gamma(0)$ for $r + is \in \mathcal{R} \cap \mathcal{D}$:

$$(6.2) \quad \Phi^r(\Gamma(is)) = \Phi^r S^s(\Gamma_0) = \Gamma(r + is) = S^s \Phi^r(\Gamma_0) = S^s(\Gamma(r)),$$

for $r + is \in \mathcal{R} \setminus \{r_0 + is_0\}$. See also (1.4).

Let $0 \leq s < s^*(r) \leq \infty$ denote the maximal forward interval of existence of the strongly continuous local Schrödinger flow $S^s(\Gamma(r))$. For $r = r_0$, we claim Schrödinger blow-up at $s^*(r_0) = s_0 < \infty$ i.e. at the upper right corner of the rectangle \mathcal{R} . Indeed $s^*(r_0) \geq s_0$, by our construction of \mathcal{R} . Suppose $s^*(r_0) > s_0$. Then $\|\Gamma(r + is)\|$ remains uniformly bounded in some neighborhood of the upper right corner $r_0 + is_0$, by lower semicontinuity of $r \mapsto s^*(r)$. Blow-up (1.5) of $r \mapsto \|\Gamma(r + is)\|$ at $r_0 = r^*(s_0)$ under Φ^r , on the other hand, shows unboundedness of $\|\Gamma(r + is_0)\|$, for $r \nearrow r_0 = r^*(s_0)$. This contradiction shows Schrödinger blow-up of $\psi(s) := \Gamma(r_0 + is)$ at $s = s^*(r_0) = s_0$, which will complete the proof.

It only remains to construct the rectangle \mathcal{R} of (6.1), with upper right corner $r_0 + is_0 \in \partial\mathcal{D}$. Clearly we will have to choose $r_0 = r^*(s_0)$. To construct s_0 , we may restrict attention to any compact interval $s \in I := [0, \hat{s}]$, where the imaginary level $s = \hat{s}$ is already known for blow-up of $r \mapsto \Gamma(r + is)$ in finite real time $r^*(s)$. The lower semicontinuous function $s \mapsto r^*(s)$ must attain its finite minimum, on some nonempty compact subset of $0 < \underline{s}_0 \in I$. Indeed, $\underline{s}_0 = 0$ does not qualify, because $r^*(0) = \infty$ on the real heteroclinic orbit $\Gamma(r)$. Define $s_0 := \min \underline{s}_0$ and $r_0 := r^*(s_0)$. Then the rectangle \mathcal{R} with upper right corner $r_0 + is_0$ satisfies (6.1).

This completes the proof of theorem 1.4. \(\boxtimes\)

7 Discussion

7.1 Overview

We conclude with a cursory collection of some additional aspects, and shortcomings, of our results. Above, we have defined blow-up in the topology of fractional power spaces X^α and H^1 Sobolev norms; see (1.5) and (1.17). In section 7.2 we show how this implies blow-up (7.3) in L^∞ sup-norm.

In section 7.3 we return to the scalar ODE case $\dot{w} = g(w)$, generalizing the introductory remarks on quadratic g of section 1.8. Detailed geometric analysis of $g(w) = w^n - 1$, for $n = 3$ and 4, explores how Masuda's example is limited to the quadratic case $n = 2$.

Based on extensive work in [FieRo20], for the real case, section 7.4 explores the boundary of the fastest unstable manifold in complex time. Blow-up and quasi-periodicity are discussed. Based on section 7.3, we do not expect global de-singularization by branched ramifications. See for example [For81, Jo06, Lam09] for terminology on Riemann surfaces.

Section 7.5 highlights a few results from the literature on PDE blow-up in the parabolic and Schrödinger settings (1.9) and (1.16), mostly for the purely quadratic case $\lambda = 0$. After due celebration of the ground-breaking and pioneering results [Mas82, Mas84] by Kyûya Masuda, we comment on exciting recent results by Jonathan Jaquette and co-workers, in some detail. As a fundamentally new tool, they have brought rigorous numerics and computer-assisted proofs to the field.

Under periodic boundary conditions in x , section 7.6 provides a glimpse at the construction of traveling wave solutions $w(s, x) = w(\xi)$ in complex time $\zeta = i(x - cs)$. Mixing real and imaginary traveling wave time as $\zeta = cr + ix$, we also construct finite time blow-up with a traveling wave flavor.

In section 7.7, we follow [Fie23] to describe the potential relevance of complex entire homoclinic orbits, even in ODEs, for the elusive phenomenon of ultra-exponentially small homoclinic splittings and ultra-invisible chaos. The existence of such homoclinic orbits remains a 1,000 € open question.

Our final section 7.8 recalls a reversible scalar ODE example of second order. The example features a non-entire homoclinic orbit, and a coexisting complex entire (in fact a cosine) periodic orbit. As a consequence, ultra-exponential homoclinic splitting may fail, but ultra-exponentially sharp Arnold tongues do occur under suitable, rapidly periodic forcing.

7.2 Blow-up in sup-norm

We show how the H^1 Schrödinger blow-up asserted in theorem 1.4 actually implies L^∞ blow-up.

To align the settings of quadratic heat and Schrödinger equations (1.9), (1.16), let $0 \leq r \nearrow r^* < \infty$ denote H^1 blow-up, analogously to (1.5), (1.17), for complex time rays $t = r \exp(i\vartheta)$ along any fixed inclined direction $|\vartheta| \leq \pi/2$. In other words, consider solutions $w(r)$ of

$$(7.1) \quad e^{i\vartheta} w_r = w_{xx} + 6w^2 - \lambda,$$

such that

$$(7.2) \quad \|w(r)\|_{H^1} \rightarrow \infty \quad \text{for } r \nearrow r^*.$$

A more standard notion requires blow-up in sup-norm, instead, i.e.

$$(7.3) \quad \limsup \|w(r)\|_{L^\infty} = \infty \quad \text{for } r \nearrow r^*.$$

We claim that the two conditions (7.2), (7.3) are equivalent, in our setting.

Indeed, standard semigroup theory and the Sobolev embedding $H^1 \hookrightarrow L^\infty$ show that (7.3) implies (7.2).

To establish the converse direction, we argue by proving the contrapositive: suppose $\|w(r)\|_{L^\infty} \leq C$ violates (7.3), remaining uniformly bounded, for $0 \leq r \leq r^*$. For classical solutions, we differentiate (7.1) with respect to x , and multiply with the conjugate complex \bar{w}_x . Integration over x , by parts, then provides the following differential inequality for the L^2 -norm $\|w_x\|_{L^2}$:

$$(7.4) \quad \frac{1}{2} \partial_r \|w_x\|_{L^2}^2 = -\cos \vartheta \|w_{xx}\|_{L^2}^2 + 12C \|w_x\|_{L^2}^2 \leq 12C \|w_x\|_{L^2}^2.$$

Note invariance of estimate (7.4) under the scaling (1.10), by a homogeneous factor n^8 . The differential inequality implies at most exponential growth, and hence uniform bounds in H^1 , for inclinations $|\vartheta| \leq \pi/2$ and $0 \leq r \leq r^*$. In weak form, the same H^1 -bound extends to mild solutions. This proves our contrapositive claim, by violation of (7.2). The same argument extends, of course, to scalar nonlinearities $g(x, w, w_x)$ with bounded derivatives, uniformly in w_x and locally uniformly in w .

With the particular choices $\vartheta = \pm\pi/2$, $r = s$, and $w = \psi$, theorem 1.4 then asserts L^∞ Schrödinger blow-up (7.3) of $\psi(s)$, and blow-down, for real $\psi(0) := \Gamma(r_0)$ and at finite times $s \rightarrow \pm s^*$.

7.3 ODEs revisited

In this section we exclude any complex entire heteroclinic, or homoclinic, orbits $\Gamma : W_- \rightsquigarrow W_+$ in the most elementary spatially homogeneous case of general scalar ODEs

$$(7.5) \quad \dot{w} = g(w).$$

Generalizing the quadratic case of section 1.8, we only assume the nonlinear vector field $g : \mathbb{C} \rightarrow \mathbb{C}$ is itself complex entire. With blow-up $w \rightarrow \infty$ established, we then desingularize $w = \infty$ for polynomial nonlinearities g .

We start with a brief folklore of some relations among Brouwer degree, residues, Poincaré linearization, and synchronous periodicity for scalar holomorphic ODEs; see e.g. [Žol06].

7.1 Proposition. *Let e denote equilibria $g(e) = 0$ of the scalar complex entire ODE (7.5), and let $w(t)$ denote nonstationary periodic orbits of minimal period $|p|$. We let $p < 0$ indicate negative, clockwise orientation of w . Positive, anti-clockwise orientation has $p > 0$. Then the following holds true:*

- (i) *The local Brouwer degree $\deg(g, e, 0)$ of any equilibrium e coincides with the algebraic multiplicity of e as a zero of g .*
- (ii) *Any periodic orbit w surrounds a single equilibrium e .*
- (iii) *The surrounded equilibrium e is algebraically simple.*
- (iv) *The signed minimal period p of w is given by $\pm 2\pi i / g'(e)$, with purely imaginary linearization $g'(e)$ at the center e .*

(v) *The interior of w is foliated by synchronous periodic orbits nested around the center e , of identical signed minimal period p .*

Proof. To prove claim (i), let $e = 0$ be a zero of $g(w) = w^n(g_n + \dots)$ with algebraic multiplicity n and some complex coefficient $g_n \neq 0$. Introduce polar coordinates $w = \varrho \exp(i\alpha)$ with small $\varrho > 0$. Then the local Brouwer degree at $g(0) = 0$ is given by the winding number n around $w = 0$ of $\alpha \mapsto g(w) = \varrho^n(g_n \exp(in\alpha) + \dots)$, for $0 \leq \alpha \leq 2\pi$. Alternatively, the winding number coincides with the residue n of $(\log g)' = g'/g$ at $w = 0$.

To prove claims (ii) and (iii), let Ω denote the interior of w . The winding number of g along any nonstationary periodic orbit $\dot{w} = g(w)$ equals 1. It also coincides with the Brouwer degree $\deg(g, \Omega, 0)$. That Brouwer degree adds up the contributions of all equilibria $e \in \Omega$. Invoking (i) proves (ii), i.e. existence, uniqueness, and simplicity of e .

To prove (iv), let e denote any simple zero of g . Then $g(w) = (w - e)(g'(e) + \dots)$ identifies $1/g'(e)$ as the residue of the reciprocal $1/g(w)$ at e . Separation of variables, on the other hand, identifies the signed real period p by integration along the time-oriented periodic orbit w as

$$(7.6) \quad p = \oint_w \frac{1}{g(w)} dw = \pm 2\pi i / g'(e).$$

Here we have used (ii) and the residue theorem, to evaluate the integral. Since p is real, $g'(e)$ is purely imaginary. The positive or negative orientation of the periodic orbit w provides the appropriate sign of p . This proves claim (iv).

We prove claim (v) for left-winding $p > 0$, without loss of generality. Analyticity of $w(r)$ extends to a narrow strip $|s| < \varepsilon$ of complex times $t = r + is$. Since the real and imaginary ODE flows commute in the strip, as in (1.4), all orbits $r \mapsto w(r + is)$ with $|s| < \varepsilon$ share the same minimal period $p > 0$. Because $\dot{w}(r) \neq 0$, the map $t \mapsto w(t)$ is locally diffeomorphic and preserves orientation. In particular, the orbits $w(t)$ with $0 < s < \varepsilon$ are nested around e in the interior Ω of the orbit $w(r)$. This shows that the region foliated by periodic orbits is open in Ω . Since Ω is also bounded by $\partial\Omega = w$, limits of periodic orbits in Ω are again periodic, or coincide with e , connectivity of the disk Ω , and (iv), imply the synchronous periodic foliation of $\Omega \setminus \{e\}$. Note how the foliation agrees with local Poincaré linearization (2.3) at e . This proves the final claim (v), and the proposition. \bowtie

Next, we keep g complex entire and consider $\Gamma : W_- \rightsquigarrow W_+$ which are heteroclinic between any two complex roots $g(W_\pm) = 0$, in real time $t = r$. We do not assume W_\pm to be simple, and we explicitly allow Γ to be homoclinic, i.e. $W_+ = W_-$. We claim $\Gamma(t)$ itself cannot be entire, in complex time t .

If W_\pm are hyperbolic, i.e. for $\operatorname{Re} g'(W_\pm) \neq 0$, the claim follows from theorem 1.1. In the possibly nonhyperbolic scalar case, again, we argue indirectly and assume Γ to be complex entire. To reach a contradiction, we first show that Γ then possesses a complex period p .

Indeed, complex periodicity follows from the great Picard theorem, as follows. Let $\Gamma_0 := \Gamma(0)$. Since heteroclinic orbits $\Gamma(t)$ cannot be polynomial, the holomorphic map $0 \neq t \mapsto \Gamma(1/t)$ possesses an essential singularity at $t = 0$. The great Picard theorem then implies

that $\Gamma(t)$ attains any complex infinitely many times, of course with the single equilibrium exception $W_+ = W_-$. In particular, the heteroclinic orbit $\Gamma(t)$ must be homoclinic to $W = W_\pm$ in real time $t = r$, with a complex period p of nonvanishing imaginary part.

We may therefore rescale time to normalize the complex period to $p = \pi i$, at the expense of “real” time rays $r \exp(i\vartheta)$, $r \geq 0$ now progressing at some fixed angle $0 < |\vartheta| \leq \pi/2$ to the imaginary time axis. By proposition 7.1, the resulting π -periodic orbits of Γ in rescaled imaginary time s are nested around the unique surrounded equilibrium, say $g(0) = 0$, foliating the punctured plane $\mathbb{C} \setminus \{0\}$ in uniformly positive orientation. Compare with figure 1.2 and proposition 7.1 (v). The nondegenerate holomorphic map Γ preserves the angle ϑ . As rescaled real time r increases along its inclined ray, therefore, the time-rescaled homoclinic orbit $r \mapsto \Gamma(r \exp(i\vartheta))$ can only proceed inwards everywhere, or else outwards, at the fixed nonzero angle ϑ with respect to the oriented periodic foliation. This contradiction to homoclinicity proves that scalar heteroclinic orbits Γ cannot be entire.

With blow-up established, we now have a closer geometric look at blow-up and blow-down of (7.5), viz. at $w = \infty$, for polynomial nonlinearities

$$(7.7) \quad \dot{w} = g(w) = w^n + \dots + g_0 = \prod_{m=0}^{n-1} (w - e_m),$$

with $n \geq 2$. We assume all zeros e_m of g to be simple. A standard example is $g(w) = w^n - 1$ with roots of unity $e_m = \exp(2\pi i m/n)$ and linearizations $g'(e_m) = n e_{-m}$, for $m \bmod n$. Standard integration as in (7.6) provides solutions

$$(7.8) \quad t = \text{const} + \frac{1}{n} \sum_{m=0}^{n-1} e_m \log(w(t) - e_m).$$

Explicit as this may be, however, it does not provide much global information on the blow-up orbits $w(t) \rightarrow \infty$ of (7.7).

Any de-singularization of (7.7), in real time $t = r$, should provide some global real flow on the Riemann sphere $\mathbb{S}^2 = \mathbb{C}_\infty = \mathbb{C} \cup \{\infty\}$, such that the orbits contain the orbits of (7.7) on $w \in \mathbb{C}$. Topologically speaking, the Lefschetz fixed point formula, or Poincaré-Hopf theorem [Zol06], then requires the local Brouwer degrees $\deg_m = \deg(g, e_m, 0) = +1$ of the simple nondegenerate equilibria $g(e_m) = 0$ to sum up with the local Brouwer degree \deg_∞ at $w = \infty$ to the Euler characteristic $\chi=2$ of the 2-sphere \mathbb{S}^2 , i.e.

$$(7.9) \quad \deg_\infty + \sum_{m=0}^{n-1} \deg_m = \deg_\infty + n = \chi = 2.$$

In particular $w = \infty$ must become an equilibrium, for $n \geq 3$, of local Brouwer degree

$$(7.10) \quad \deg_\infty = 2 - n < 0.$$

Proposition 7.1 (i), in particular, excludes holomorphic de-singularization at $w = \infty$.

To de-singularize (7.7), more explicitly, let $z = 1/w$ and multiply the ODE for z by $|z|^{2(n-2)}$, i.e.

$$(7.11) \quad |z|^{2(n-2)} \dot{z} = -\bar{z}^{n-2} (1 + \dots + g_0 z^n).$$

We have lost complex analyticity, but retained real analyticity, on the right hand side. On the left, we obtain a nonzero positive Euler multiplier $|z|^{2(n-2)}$, outside the singularity $z = 0$, alias $w = \infty$. Omission of the multiplier preserves orbits, in real time. For $z \neq 0$, we therefore replace (7.12) by the real analytic equation

$$(7.12) \quad \dot{z} = \tilde{g}(z) := -\bar{z}^{n-2}(1 + \dots + g_0 z^n).$$

For Masuda's quadratic case $n = 2$, the vector field becomes regular nonzero at $z = 0$. For $n \geq 3$, in contrast, we introduce an equilibrium at $z = 0$. Note $\deg_\infty = n - 2$ is given by the local winding number of the vector field (7.12) at $z = 0$. This agrees with our abstract consideration (7.10). For $n = 3$, the equilibrium $z = 0$ is hyperbolic of local degree $\deg_\infty = -1$. The unstable and the stable manifolds separate the plane into four hyperbolic sectors, locally. In the following, see figure 7.1 for an illustration of this special case $n = 3$, and of $n = 4$.

For general $n \geq 3$, we introduce polar coordinates $z = \varrho \exp(i\alpha)$:

$$(7.13) \quad \dot{\varrho} = \varrho(-\cos((n-1)\alpha) + \dots);$$

$$(7.14) \quad \dot{\alpha} = \sin((n-1)\alpha) + \dots$$

Here we have vested (7.12) with yet another Euler multiplier ϱ^{-n+3} , and we have omitted higher order terms in ϱ . This “blow up” at $z = 0$, in the sense of singularity theory, replaces $w = \infty$ by the circle $\varrho = 0$, $\alpha \in \mathbb{S}^1$. In other words, polar coordinates compactify $\mathbb{C} = \mathbb{R}^2$ to the closed unit disc; see figure 7.1. On the invariant boundary circle $\varrho = 0$, a total of $2(n-1)$ hyperbolic equilibria $\alpha_k = \pi k / (n-1) \in \mathbb{S}^1$ appear, for $k \bmod 2(n-1)$. In figure 7.1 (a) and (c), we label the equilibria at α_k by \mathbf{k} . Within the boundary circle, they are alternatingly unstable, at even \mathbf{k} , and stable, at odd \mathbf{k} . Their corresponding stable and unstable counterparts, received from and sent into $|w| = |1/z| < \infty$, are marked red and blue, respectively. In (7.7), they mark red blow-up and blue blow-down of $w(t)$, in finite real original time t . In (7.12), they also delimit the $2(n-1)$ local hyperbolic sectors of the equilibrium $z = 0$, according to the planar classification by Poincaré. See section VII.9 in [Har02], and (b), (d) of figure 7.1. In (b), i.e. for $n = 3$, red and blue simply mark the $2(n-1)$ half branches of the stable and unstable manifolds at the hyperbolic equilibrium $z = 0$ of (7.12).

Based on $\dot{w} = g(w) = w^n - 1$, it is an easy exercise to obtain the global planar phase portraits of figure 7.1 under real-time flows $t = r \in \mathbb{R}$, at least for $n = 3, 4$. We recall invariance of the boundary circle $\alpha \in \mathbb{S}^1$ at $w = \infty$, with $2(n-1)$ alternating hyperbolic saddles \mathbf{k} . Since the polynomial g has real coefficients, complex conjugation provides a symmetry of upper and lower half planes. Indeed $w(t)$ solves (7.7), if and only if $\bar{w}(t)$ does. In particular the horizontal real axis is invariant. This determines the horizontal separatrices of the boundary equilibria $\mathbf{k} = \mathbf{0}, \mathbf{n} - \mathbf{1}$, and the real blow-up trajectories of e_0 . Note how the real heteroclinic orbit $e_0 \rightsquigarrow e_{n/2}$ is linked to, both, real blow-up $e_0 \rightsquigarrow \mathbf{0}$ and to real blow-down $\mathbf{n} - \mathbf{1} \rightsquigarrow e_{n/2}$, for even n and in complex time. For odd n , blow-up $e_0 \rightsquigarrow \mathbf{0}$ and $e_0 \rightsquigarrow \mathbf{n} - \mathbf{1}$ occurs in both real directions. By symmetry, it remains to study the upper half plane $v > 0$ of $w = u + iv$.

Consider the case $n = 3$ of figure 7.1 (a), (b), first. The absence of center equilibria excludes periodic orbits; see proposition 7.1 (iv). The Poincaré-Bendixson theorem [Har02]

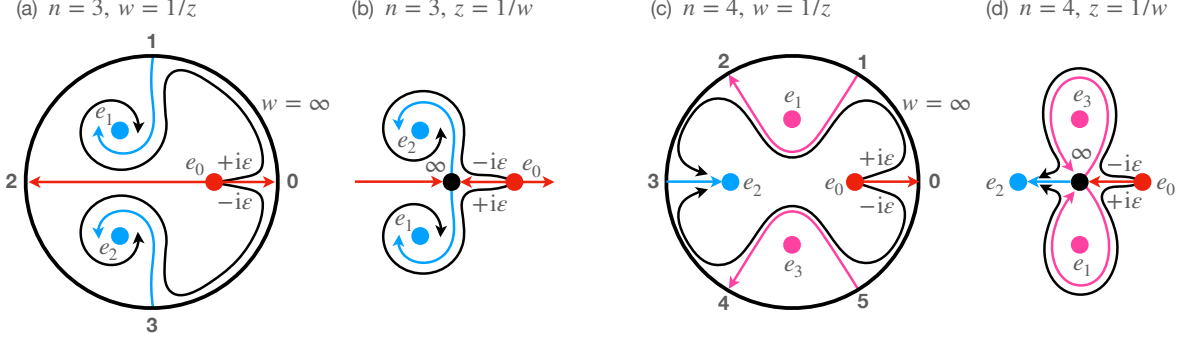


Figure 7.1: Schematic phase portraits, in real time, of complex-valued ODEs (7.7), (7.12) – (7.14) based on $\dot{w} = w^n - 1$. For $n = 3$ see w in (a), and $z = 1/w$ in (b). Similarly, w in (c) and $z = 1/w$ in (d) refer to $n = 4$. The invariant circle $\varrho = |z| = 0$, $\alpha \in \mathbb{S}^1$ at $w = \infty$ is marked black in (a), (c). Equilibria e_m are stable (blue), centers (purple) surrounded by periodic orbits, or unstable (red). Unstable blow-down separatrices (blue) emanate from $w = \infty$, alias $z = 1/w = 0$, at odd-labeled vertices $\mathbf{k} = 1, 3, 5$. Stable blow-up separatrices (red) run towards the even-labeled saddles $\mathbf{k} = 0, 2, 4$. In (c), two pairs of separatrices coincide (purple) in the heteroclinic separatrices $1 \rightsquigarrow 2$ and $5 \rightsquigarrow 4$. The black trajectories marked $\pm i\varepsilon$ are complex perturbation of the red real blow-up trajectories $e_0 \rightsquigarrow 0$, say with initial conditions $w(0) = 2 \pm i\varepsilon$. For $n = 3$ in (a), they closely follow the heteroclinic chains $e_0 \rightsquigarrow 0 \rightsquigarrow 1 \rightsquigarrow e_1$ and $e_0 \rightsquigarrow 0 \rightsquigarrow 3 \rightsquigarrow e_2$, respectively. The intermediate heteroclinic parts $0 \rightsquigarrow 1$ and $0 \rightsquigarrow 3$ on the invariant boundary circle \mathbb{S}^1 concatenate initial red blow-up to terminal blue blow-down. In the polar view (b), centered at $w = \infty$, $z = 0$, the boundary parts are conflated into $z = 0$. Note the markedly distinct limits of the two perturbations, for $\varepsilon \searrow 0$, given by the two distinct remaining blow-up-down concatenations $e_0 \rightsquigarrow \infty \rightsquigarrow e_1$ and $e_0 \rightsquigarrow \infty \rightsquigarrow e_2$. In case $n = 4$ (d), the initial red blow-up and terminal blue blow-down limits of both perturbations $\pm i\varepsilon$ coincide. Each limit $e_0 \rightsquigarrow \infty \rightsquigarrow \infty \rightsquigarrow e_3$, however contains an additional purple blow-down-up part $\infty \rightsquigarrow \infty$ (purple) which is homoclinic to $z = 0$. The two purple homoclinic orbits, however, are markedly distinct: their lobes surround the distinct centers e_1 and e_3 , respectively, in opposite orientation. In (c), this is manifested by the two purple heteroclinic saddle-saddle orbits $1 \rightsquigarrow 2$ and $4 \rightsquigarrow 3$. Together with the heteroclinic orbits on the black invariant boundary circle \mathbb{S}^1 which run between the same saddles, in opposite direction, we obtain two heteroclinic loops, properly foliated by synchronous periodic orbits around the centers e_1 and e_3 as in proposition 7.1 (v).

therefore identifies e_1 as the only possible ω -limit set of the blue blow-down separatrix of **1** in the upper half plane. All remaining trajectories w in the open upper half plane are heteroclinic of type $e_0 \rightsquigarrow e_1$.

In case $n = 4$ of figure 7.1 (c), we encounter time reversibility for $g(w) = w^n - 1$ and any even n . The time reversor is horizontal reflection at the vertical imaginary axis. Indeed, $w(t)$ solves (7.5), whenever $-\bar{w}(-t)$ does. Therefore, the center equilibria $e_1, e_3 = \pm i$ are locally surrounded by periodic orbits, only, up to the purple saddle-saddle blow-down-up orbits $1 \rightsquigarrow 2$ and $5 \rightsquigarrow 4$. In fact, the unstable blow-down separatrix of **1** (usually blue, here purple) has to cross the imaginary axis $\text{Re } w = 0 < \text{Im } w$. Indeed, the first quadrant $\{\text{Re } w > 0, \text{Im } w > 0\}$ does not contain equilibria and, therefore, cannot contain periodic orbits. See proposition 7.1 (ii). Reflecting on the first crossing, say at time $t = 0$, reversibility implies that the unstable blow-down separatrix has to coincide with the stable blow-up separatrix of **2**, usually colored red. We have therefore colored the resulting saddle-saddle heteroclinic orbit $1 \rightsquigarrow 2$ purple. Similar arguments show that the resulting heteroclinic loop between **1** and **2** is filled with periodic orbits around the

center e_1 . (Without reversibility, see also proposition 7.1 (v).) In (d), i.e. upon the identification of the boundary circle $\varrho = |z| = 0$, $\alpha \in \mathbb{S}^1$ with $w = \infty$, the heteroclinic loops become homoclinic to $z = 1/w = 0$. The homoclinic lobes, remain foliated by a family of synchronous periodic orbits, as in proposition 7.1 (v). Indeed their minimal periods, in original time and prior to any rescaling, all coincide. The periodic family is unbounded in $w = 1/z$. All remaining trajectories w in the open upper half plane are again heteroclinic, of type $e_0 \rightsquigarrow e_2$.

The relevance of figure 7.1 is the behavior of the global trajectories $w = \Gamma_{\pm\varepsilon}$ under slight perturbations $w(0) = 2 \pm i\varepsilon$, $\varepsilon \searrow 0$, of the real blow-up initial condition $w(0) = 2$. In the case $n = 3$ of figure 7.1 (a), the heteroclinic trajectory $w = \Gamma_{+\varepsilon} : e_0 \rightsquigarrow e_1$ in the upper half plane is labeled by $+i\varepsilon$ (black). For small $\varepsilon > 0$, it closely follows the concatenated heteroclinic chain $e_0 \rightsquigarrow \mathbf{0} \rightsquigarrow \mathbf{1} \rightsquigarrow e_1$. The trajectory $\Gamma_{-\varepsilon}$ in the lower half plane, in contrast, labeled $-i\varepsilon$, closely follows the *different* concatenation $e_0 \rightsquigarrow \mathbf{0} \rightsquigarrow \mathbf{3} \rightsquigarrow e_2$. In other words, the red blow-up

The polar view of (b), centered at $w = \infty$ alias $z = 1/w = 0$, conflates the boundary circle $\varrho = |z| = 0$, $\alpha \in \mathbb{S}^1$ to a single point. This shortens the black trajectories $\Gamma_{\pm\varepsilon}$ to perturbations of the two *distinct concatenations* $e_0 \rightsquigarrow \infty \rightsquigarrow e_1$ and $e_0 \rightsquigarrow \infty \rightsquigarrow e_2$. In the limit $\varepsilon \searrow 0$, this amounts to a shared red blow-up $e_0 \rightsquigarrow \infty$ followed by two different subsequent blue blow-down orbits $\infty \rightsquigarrow e_1$ and $\infty \rightsquigarrow e_2$. This is in marked contrast to the case $n = 2$ of figure 1.2, where both approximations to the cyan blow-up orbit $1 \rightsquigarrow \infty$ continued along *the same* cyan blow-down $\infty \rightsquigarrow -1$. Since this happens in finite original time $w(t)$, the Masuda paradigm of complex near-recovery for near-homogeneous PDE solutions, after real blow-up, turns out to be a peculiarity of the quadratic case $n = 2$.

The case $n = 4$ of figure 7.1, (d) leads to heteroclinic perturbations $w = \Gamma_{\pm\varepsilon} : e_0 \rightsquigarrow e_2$ which, at least formally, seem to limit onto identical concatenations $e_0 \rightsquigarrow \infty \rightsquigarrow \infty \rightsquigarrow e_2$, for $\varepsilon \searrow 0$. Both limits share the initial red blow-up part $e_0 \rightsquigarrow \infty$ and the terminal blue blow-down part $\infty \rightsquigarrow e_2$. The two purple homoclinic blow-down-up orbits $\infty \rightsquigarrow \infty$, however, remain distinct. The limiting homoclinic loop part of $+i\varepsilon$ of $\Gamma_{+\varepsilon}$ contains the center equilibrium e_1 in its interior, whereas $-i\varepsilon$ of $\Gamma_{-\varepsilon}$ contains the center equilibrium e_3 , along with their obligatory lobes filled by counter-rotating periodic orbits. Again, these perturbations run against the quadratic Masuda paradigm. The observed discrepancies between $\Gamma_{\pm\varepsilon}$ run deeper than “mere technical” PDE difficulties which arise from the absence of a heat semiflow in reverse time $r = \text{Re } t < 0$. In fact they amount to non-unique complex continuation of homogeneous blow-up itself, in finite real time.

Our discussion pinpoints how complex blow-up leads to intriguing questions, even in the spatially homogeneous scalar ODE case of a single complex dimension which looks so boringly explicit, at first sight of (7.8). Where (7.8) suggests to view complex time t as logarithmically ramified over w at the equilibria $w = e_m$, the above study of $z = 1/w$ rather suggests to, conversely, view $z = 0$ as a ramification point of order $n - 1$ over t . See [For81, Jo06, Lam09] again, for terminology. The Lefschetz formula (7.10) and proposition 7.1 (i), however, discourage any global holomorphic ramification based on equilibria of positive Brouwer degree, alone. A global classification of ODE (7.7) in the spirit of figure 7.1, up to orbit equivalence in real time, remains open. Even the case of

polynomials g with simple zeros cannot be called settled, as along as simple examples like $g(w) = w^n - 1$ are largely unexplored, geometrically and combinatorially.

7.4 Closure and boundaries of unstable manifolds

Let $\partial W^u := \text{clos } W^u \setminus W^u$ denote the topological boundary of unstable manifolds W^u . Before we return to complex time $t = r + is$, let us consider dissipative gradient-like flows in real time $t = r$ for a moment. For some of the intricacies, like Alexander horned spheres which already arise in three-dimensional settings, see the appendix by Laudenbach in [BiZh92], and the references there. Generalizations

$$(7.15) \quad u_r = u_{xx} + g(x, u, u_x)$$

of the complex quadratic heat equation (1.9) have been studied in [FieRo20], for real u rather than complex $w = u + iv$. Under our usual Neumann boundary conditions, the dynamics is gradient-like. Growth assumptions on g ensure dissipativeness and the existence of a global attractor which consists of equilibria and their heteroclinic orbits, only. For hyperbolic equilibria $u = U(x)$, transversality of stable and unstable manifolds holds automatically. In fact, the decomposition of the global attractor into the disjoint union of unstable manifolds $W^u(U)$ turns out to be a regular cell complex. The cell boundaries ∂W^u themselves possess signed hemisphere decompositions. Based on heteroclinic orbits $U = U_n \rightsquigarrow U_0$ in $W^u(U_m)$, that hemisphere decomposition is governed by cascades $U_n \rightsquigarrow U_{n-1} \rightsquigarrow \dots U_m$ of intermediate heteroclinic orbits. Here the Morse indices $i(U_k) = k$ in the cascade drop by 1 at each heteroclinic step. See [FieRo20] for further details.

For the complex quadratic heat equation (1.9), alas, the boundaries ∂W^u of unstable manifolds are not as easily described. To simplify matters, we discuss heteroclinic orbits $\Gamma : W_- \rightsquigarrow W_+$ emanating from the fastest unstable manifold W^{uu} of dimension $d = 1$ again; see section 1.7. The spatially homogeneous source equilibrium $W_- = W_\infty$ leads to spatially homogeneous fastest Γ , as discussed in sections 1.8, 7.3 above. In contrast to our ODE results for higher order polynomial nonlinearities g , [COS16] have conjectured blow-up at isolated branching singularities, in the technically similar, purely quadratic setting $\lambda = 0$ of 1-periodic boundary conditions, and based on numerical evidence; see also [FaKW22].

Locally near any non-homogeneous source $W_- = W_n$, and therefore globally, the complex extension of the fastest heteroclinic orbit $\Gamma : W_n \rightsquigarrow W_0$ in W^{uu} still parametrizes $W^{uu} \setminus \{W_-\}$. By Poincaré linearization (2.3), in fact, $z := \exp(\mu_0 t)$ parametrizes $W^{uu} \setminus \{W_n\}$, with imaginary period $p = 2\pi i / \mu_0$ and removable singularity W_n at $z = 0$. Here $t = r + is \in \mathbb{C}$, with sufficiently negative real part r .

At the spatially homogeneous, asymptotically stable target $W_+ = W_0$ of $\Gamma(r)$, matters look quite different. Comparing with (1.19), we will first notice how $\Gamma(r + is)$ fails to be p -periodic, in the imaginary time direction s and for fixed large positive r . This failure is due to blow-up at intermediate real parts r , and will occur for all but a discrete set of parameters λ . In particular, the semiflows Φ^r and Φ^{ip} fail to commute on Γ : our previous

statement (2.2) concerning commutativity was due to our indirect, and ultimately false, assumption of a complex entire heteroclinic orbits Γ .

We fill in a few details on the absence of imaginary periods ip of Γ , near W_+ . Rescaling (1.10) allows us to restrict to the case $n = 1$ of $W := W_- = W_1$, $\lambda \geq \lambda_{10} = \frac{2}{3}\pi^4$; see (1.14). In real time $t = r \nearrow +\infty$, the asymptotics of $\Gamma \rightarrow W_+ = W_0$ is well-understood; see for example [BrFie86]. With purely trigonometric eigenfunctions $c_k = \cos(2\pi kx)$, eigenvalues

$$(7.16) \quad \mu_{+,k} = -2\sqrt{6\lambda} - k^2,$$

and with the homogeneous target $W_+ = W_0 = -\sqrt{\lambda/6}$ shifted to zero, we obtain

$$(7.17) \quad \Gamma(r) = \exp(\mu_{+,0} r) + o$$

in H^1 -norm. We have also shifted real time r , appropriately. For $r \nearrow +\infty$, the error term “ o ” decays of higher order than any negative exponential rate between $\mu_{+,0} < 0$ and $\mu_{+,1} < \mu_{+,0}$. In imaginary time direction s , we may compare the Schrödinger flow $S^s = \Phi^{is}$ with the linearized flow at the target W_+ . Uniformly for bounded s , we obtain the same estimate for the complex continuation

$$(7.18) \quad \Gamma(r + is) = \exp(\mu_{+,0}(r + is)) + o.$$

On the other hand, we may invoke p -periodicity of $s \mapsto \Gamma(r + is)$ at the source W_- , as established in (1.19) for large negative r . By analytic continuation in r , at fixed $s = p$, this clashes with the r -asymptotics (7.18), unless $\exp(\mu_{+,0} ip) = 1$. In particular, Φ^r and Φ^{ip} fail to commute on Γ , for large $r > 0$, unless the global resonance condition

$$(7.19) \quad \mu_{+,0} + m\mu_0 = 0,$$

happens to hold true, for some integer $m > 0$. At the pitchfork bifurcation $\lambda = \lambda_{1,0}$ of $W = W_n$, for $n = 1$, we have already obtained the expansions

$$(7.20) \quad \mu_0 = 4\pi^2(1 + 264h^2 + \dots) > 0$$

$$(7.21) \quad \mu_{+,0} = -4\pi^2(1 + 120h^2 + \dots) < 0$$

along the branch parameter h . For (7.20), see (4.12), (4.13), (4.15), with $n = 1, k = 0$. For (7.21), see (7.16) and (3.11). This prevents global resonance (7.19): locally at pitchfork bifurcation $\lambda = \lambda_{1,0} = \frac{2}{3}\pi^4$, and hence everywhere, up to a discrete set of resonant parameters λ .

For rationally independent eigenvalues $\mu_{+,0}, \mu_{+,1}$, linearization at the target W_+ hints at yet another complication concerning the closure, and the boundary ∂W^{uu} , of the fastest unstable manifold W^{uu} generated by the heteroclinic orbit Γ . When both components are present, the resulting quasi-periodicity (or almost-periodicity) in imaginary time may cause dense orbits $\Gamma(r + is)$ in tori, for any $r > 0$ fixed large enough. In the more specific second order ODE setting (7.34), this problem will return below in the guise of traveling wave solutions in imaginary time.

Above, we have considered the fastest unstable manifold at W_- , to fix a unique heteroclinic orbit $\Gamma : W_- \rightsquigarrow W_+$. This has selected a unique complex one-dimensional object $t \mapsto \Gamma(t)$ for maximal analytic continuation. Generated by other real analytic heteroclinic orbits $r \mapsto \Gamma(r)$, many more candidates are left to explore. For example, heteroclinic orbits between equilibria of adjacent Morse indices, $i(W_+) = i(W_-) - 1$, are known to be unique in the real case [BrFie88]. More generally, Wolfrum has selected unique one-dimensional $\Gamma(r)$, characterized by constant zero number $z(\Gamma(r) - W_\pm) = z(W_- - W_+)$, whenever there exists any real heteroclinic orbit $W_- \rightsquigarrow W_+$; see [Wol02, FieRo20]. Above, we have only addressed the very special case $z = 0$. Even under spectral non-resonance at W_- , Poincaré linearization (2.3) will only assert $s \mapsto \Gamma(r + is)$ to be quasi-periodic, as well, say for $r \leq 0$, rather than periodic. The global complex geometry of such Γ , and their closure, therefore remains open.

7.5 Schrödinger and parabolic singularities

We discuss some of the previous literature on parabolic and Schrödinger blow-up, in finite complex time.

The updated standard mathematical PDE monograph on *real time* is [QS19]. Topics include multi-dimensional space, nonlinearities combining u^p and $(\nabla u)^q$, and PDE systems. In addition to the standard PDE arsenal of weak versus strong solutions and Sobolev embeddings, methods are basically a combination of three ingredients: the variational structure of energy and Lyapunov functionals, comparison and maximum principles, and – at least locally and for homogeneous nonlinearities like $\lambda = 0$ – self-similar scalings (1.10) by arbitrary $0 < n \in \mathbb{R}$. Marek Fila figures prominently, in this monograph alone, with 25 of his papers.

Consider the purely quadratic real parabolic system (1.9) with $\lambda = 0$, for the real and imaginary parts of $w = u + iv$. Restricted to real time, but for real m -dimensional x , this case has been addressed in [GNSY13] with complete mathematical rigor. The variational structure is lost, except in the invariant real subspace $v \equiv 0$. Benefitting from equal diffusion in the components u and v , however, comparison principles remain applicable. Together with self-similarity, and for certain initial conditions, this provides dichotomies between global existence, and blow-up in finite real time.

A very accessible survey on real-time blow-up phenomena of complex-valued ODEs and PDEs, in a similar spirit, is [KSK17]. It is aimed at a broad audience, with a strong emphasis on applications and numerical simulations.

What is usually “forgotten” in the above approaches, or at least ignored, are the subtle relations among real-time solutions $r \mapsto w(r + is)$, for various fixed s . These relations are induced and encoded by their contingency under commuting local flows, or semiflows, in imaginary time is . Besides the kinship between the quadratic heat and Schrödinger equations (1.9) and (1.16) which we have explored above, this is a structure worthwhile of mathematical study, as such, even when a direct interpretation of imaginary time remains elusive, “in nature”.

In the simplest, and not quite typical, case of homogeneous solutions, the orange periodic circles of figure 1.2, in imaginary time, illustrate such isochronous contingency which globally synchronizes the orthogonal blue heteroclinic orbits, in real time. And vice versa. See also our discussion in sections 7.3, 7.4 above and, in particular, the synchronicity of nested periodic orbits in proposition 7.1 due to the residue theorem.

Forty years ago, Kyûya Masuda has started a systematic study of blow-up in *complex time* with his pioneering work on the purely quadratic heat equation (1.9) at parameter $\lambda = 0$, and in any space dimension. Under Neumann boundary conditions, elliptic maximum principles imply that $u \equiv 0$ is the only real equilibrium. For almost homogeneous real initial conditions $0 \leq w_0 \not\equiv 0$, Masuda was able to circumvent blow-up, at real time $0 < r = r^*(w_0) < +\infty$, via a sectorial detour in complex time $t = r + is$. See [Mas84] for proofs, and the earlier announcement [Mas82]. Notably, he also showed that the detours via positive and negative imaginary parts s agree in their real overlap after blow-up, if and only if u_0 is spatially homogeneous.

More than three decades after these amazing results, [COS16] pointedly remarked:

Masuda’s pioneering work does not seem to have a follower. ... His paper seems to be a good example of a paper of high originality with few citations. It seems to us that, although there are numerous papers studying blow-up of solutions of nonlinear parabolic equations, few investigate singularities in the complex t -plane.

For some further references in the context of the notoriously difficult Navier-Stokes and Euler PDEs, as well as complex x and vorticity ODEs, see [COS16] again. The most diligent monograph on blow-up in real time, [QS19], kindly mentions [Mas84], in passing, for his complex circumvention of “complete” real-time blow-up; see the short remark 27.8(f).

In one space dimension, Stuke has addressed the Masuda setting under Dirichlet boundary conditions [Stu17, Stu18]. Even though Stuke’s setting is quite similar to Masuda, the required techniques are quite different. Masuda exploited the homogenous ODE solution. In the one-dimensional fastest unstable manifolds, Stuke detected how heteroclinic orbits, blow-up, and center manifolds in real time are related, via complex time. In the case of the semilinear heat equation, a trapping argument similar to [GNSY13] showed that blow-up must occur on the real time axis. This led to the paradigm of the present paper. For the quadratic heat equation, the results also added to Masuda’s attempts at a circumnavigation of real-time blow-up, via the complex time-domain. Continuation was pursued, separately, in the upper complex half plane $s > 0$, and in the lower half plane $s < 0$. Return to the real axis was achieved, only, after a finite slit interval of real times r trailing $r = r^*$. The fact that the continuations do not match after blow-up was seen as caused by the ratio of asymptotic eigenvalues at the heteroclinic equilibria W_{\pm} . Attempts to reduce the trailing slit interval to the singleton $\{r^*\}$, i.e. to identify blow-up as an isolated singularity in complex time as conjectured by [COS16], have failed so far, even on the rather formal level of matched asymptotic expansions [FaKW22].

Jonathan Jaquette and co-authors mostly addressed the purely quadratic case $\lambda = 0$ of the Schrödinger equation (1.9). Spatial periodicity $x \in \mathbb{T}^m$ is imposed. By reflection through the boundary, Neumann boundary conditions can be subsumed.

The Schrödinger equation (1.16) on \mathbb{T}^m is integrated in [Jaq21], by explicit recursive ODEs for the spatial Fourier-coefficients. The one-dimensional case $m = 1$ with monochromatic initial condition $\psi_0(x) = a \exp(2\pi i x)$ and spatial period 1 is studied in detail. Solutions $\psi = \psi(s, x)$ of (1.16) are shown to be explicitly time-periodic of minimal period $p = 1/(2\pi)$, alias frequency $(2\pi)^2$, for $|a| \leq 2\pi^2$. For $|a| \geq 4\pi^2$, in contrast, blow-up occurs in finite “real” time s . In higher dimensions $m > 1$, small solutions are shown to be quasi-periodic in time s . To avoid small divisors, initial conditions ψ_0 are assumed to be supported on strictly positive spatial Fourier modes. The fundamental frequencies $\Omega_j = \omega_j^2$ in time s originate from the spatial frequencies ω_j , alias spatial periods $q_j = 2\pi/\omega_j$, of \mathbb{T}^m imposed in the spatial directions x_j , for $j = 1, \dots, m$. From our abstract point of view, these results fit well with an elusive partial Poincaré linearization of (1.9), within the infinite-dimensional strong stable manifold W^{ss} of the trivial equilibrium $W \equiv 0$ at $\lambda = 0$.

As an alternative to the above analysis, an approach based on rigorous numerics is pursued in the trilogy [JLT22a, JLT22b, TLJO22]. We proceed chronologically.

Rigorous numerics, in the spirit of previous analysis by [Mas82, Mas84, Stu17, Stu18], has been provided in [TLJO22]. The setting is the purely quadratic heat equation (1.9), $\lambda = 0$, under 1-periodic boundary conditions in $m = 1$ spatial dimensions. Specifically, they follow [COS16] for the large real initial condition $w_0 = 50(1 - \cos(2\pi x))$. Corroborating [COS16], they rigorously provide a box, in complex time, where a complex singularity of Masuda type has to occur. They also consider the inclined Schrödinger-like equation (7.1), i.e. (1.9) along rays $t = r \exp(i\vartheta)$, $r \geq 0$. Under the same initial condition w_0 , in contrast, they prove global existence, and convergence $w(r) \rightarrow 0$ for $r \nearrow \infty$, at fixed angles $\vartheta \in \{1, 2, 3, 4\} \cdot \pi/12$. A second conjecture in [COS16] aims at such a result for $\vartheta = \pi/2$, i.e. for the Schrödinger case (1.16), and any initial condition $\psi_0 \in L^2$. The counterexamples of our theorem 1.4, of course, require $\lambda > 0$ rather than $\lambda = 0$.

The purely quadratic Schrödinger case (1.16), $\lambda = 0$, is also studied in [JLT22a]. We comment, specifically, on the nontrivial complex equilibria u_1^i and u_1^{ii} of [JLT22a], Theorem 1.7, figure 1, in line with their open question 6.4. The result is also reproduced in [JLT22b]. Both equilibria can indeed be obtained analytically, along the completely classical lines of our section 3. Consider $g_2 = 0$ in (3.8), with discriminant $\Delta = -27g_3^2$ and Klein-invariant $J = 0$. The corresponding hexagonal period lattice Λ in (3.3) is characterized uniquely by the modular parameter $\tau := \exp(\pi i/3)$, alias purely imaginary $h = \exp(\pi i\tau) = i \exp(-\frac{\pi}{2}\sqrt{3})$ in (3.12), (3.13). Under Neumann boundary conditions at minimal spatial half-period $1/2$, we obtain the equilibrium

$$(7.22) \quad u_1^i(x) = 6 W_1(x) := -6 \wp(x + \tfrac{1}{2}\tau).$$

Families $W_{\pm n}$ arise, because the parameter $\lambda = 0$ is not affected by the self-similar rescalings (1.10).

Seeking complex solutions for $\lambda = 0$, we can utilize the more general invariance of the equilibrium equation (3.1), i.e. of $W_{xx} + 6W^2 = 0$, under any complex scaling factor $\sigma \in \mathbb{C}$. This generates equilibrium families

$$(7.23) \quad W^\sigma(x) := \sigma^2 W(\sigma x + z_0),$$

for suitably chosen σ and z_0 . The equilibrium $u_1^{ii}(x)$ of [JLT22a] is an example. Explicitly, $u_1^{ii}(x) = -6\wp^\sigma(x)$ along the line segment $z = \sigma x + z_0$, $0 \leq x \leq \frac{1}{2}$, with rescaling factor $\sigma = \sqrt{3}\exp(\pi i/6)$ and offset $z_0 = \frac{1}{2}\tau$. In other words,

$$(7.24) \quad u_1^{ii}(x) = -6\sigma^2 \wp(\sigma x + \tfrac{1}{2}\tau).$$

More generally, proper complex scaling produces complex Neumann equilibria W^σ from \wp , evaluated on line segments between points z_0 and $z_0 + \frac{1}{2}\sigma$ of the half-period lattice $\frac{1}{2}\Lambda$. The segments have to avoid the singularities of \wp on Λ itself, of course. The solution $u_1^{ii}(x)$, for example, is based on the segment from $z_0 = \frac{1}{2}\tau$ to $\tau + \frac{1}{2}$. The solution $u_1^i(x)$ runs horizontally, from $z_0 = \frac{1}{2}\tau$ to $\frac{1}{2}\tau + \frac{1}{2}$. Explicit Fourier expansions (3.12), (3.13) of $\pm\wp$ apply. It is an elementary, but worthwhile, task to explicitly enumerate all possibilities on the hexagonal lattice.

Under periodic boundary conditions, and even before invoking any rescalings σ , we obtain a full 2-torus of primary complex equilibria $W(x) = -\wp(x + z_0)$. Only shifts by real $z_0 \in \mathbb{T}^2 = \mathbb{C}/\Lambda$ correspond to spatial shifts of $x \in \mathbb{T}^1 = \mathbb{R}/\mathbb{Z}$. The exceptional solution for real z_0 is spatially quadratically singular at $x = 0$, of course. Complex scalings σ also apply.

Remarkably, computer-assisted proofs establish the existence of heteroclinic PDE orbits between $W \equiv 0$ and the two nontrivial equilibria $W = u_1^i, u_1^{ii}$. See [JLT22a], theorem 1.9 and, for u_1^i , also figure 2. The heteroclinic orbits then run in either direction, due to a reversibility (7.25) akin to (1.18). In addition, their theorem 1.5 presents an open set of small homoclinic PDE solutions to $W_\infty := 0$, with exponentially decaying Fourier modes.

Since the equilibria u_1^i, u_1^{ii} are not real, reversibility (1.18) is adapted here as follows. We first note that $\psi(s, x)$ solves the quadratic Schrödinger equation (1.16), also, if and only if

$$(7.25) \quad (R\psi)(s, x) := \bar{\psi}(-s, \tfrac{1}{2} - x)$$

does. As always, the parameter $\lambda = \bar{\lambda}$ is assumed to be real, here. For the purely quadratic case $\lambda = 0$ of the Schrödinger equation (1.16), we note R -invariance $RW = W$, for any equilibrium $W \in \{0, u_1^i, u_1^{ii}\}$.

Now assume $\Gamma : W_- \rightsquigarrow W_+$ is heteroclinic, for any $W_\pm \in \{0, u_1^i, u_1^{ii}\}$. Then R -invariance of W_\pm , and time reversibility of Γ under R , imply that the heteroclinic orbit $R\Gamma : W_+ \rightsquigarrow W_-$ runs in the opposite direction. Similar observations, with or without spatial reflection, apply to complex equilibria for general real nonlinearities $\bar{g}(w) = g(\bar{w})$ replacing purely quadratic $g(w) = w^2$.

For complex entire nonlinearities, intriguing questions concern blow-up of complex time extensions $\Gamma(s - ir)$, alias solutions $\Gamma(r + is)$ of nonlinear heat equations like (1.9). For the

purely quadratic heat equation (7.1) with $\lambda = 0$ and inclined time rays $t = r \exp(i\vartheta)$, $r \geq 0$, the spectrum and complex two-dimensional unstable manifold of W_1 are beautifully explored in [JLT22b]. Inclinations ϑ are chosen in $\{0, 1, 2\} \cdot \pi/4$. The complex eigenspace of one of the two complex conjugate unstable eigenvalues (at $\vartheta = 0$) is probed for computationally rigorous heteroclinic orbits $\Gamma : W_1 \rightsquigarrow 0$, in angular rays of 1° steps. Results document existence, as well as absence, of Γ , depending on time inclination ϑ and angular degree of departure from W_1 . For $\vartheta = 0$ or $\pi/4$, blow-up in r is observed in the unstable manifold of W_1 . Such advanced insights and inspiring results concerning non-real complex equilibria, and the cases $\lambda \leq 0$, certainly lead beyond our present focus on real equilibria. With our undue present constraints yet to overcome, like hyperbolicity, fast unstable manifolds, nonresonance, and asymptotically stable targets, it may require substantial further analysis to progress towards such more complex directions, with all due diligence and generality.

7.6 Periodic traveling waves in complex time

In this section, we start from the parabolic PDE under p -periodic boundary conditions:

$$(7.26) \quad w_r = w_{xx} + w^2 - 1, \quad x \in \mathbb{S}^1 = \mathbb{R}/p\mathbb{Z}.$$

Up to positive scaling, this addresses the quadratic case (1.9); generalizations to general complex entire “pendulum” nonlinearities g are evident. On the whole real line $x \in \mathbb{R}$, *real traveling wave solutions* $w(r, x) = W(\xi) \in \mathbb{R}$, in the real traveling wave coordinate

$$(7.27) \quad \xi = x - cr,$$

have been studied, ever since pioneering work by Fisher, Kolmogorov and coworkers [Fish1937, KPP1937]. For a survey of further developments in real settings, much beyond this first, standard variant and including PDE stability, see for example [San02]. Denoting $' = \frac{d}{d\xi}$, traveling waves $w = W(\xi)$ arise from global solutions of the ODE

$$(7.28) \quad W'' + cW' + W^2 - 1 = 0.$$

For positive wave speeds $c > 0$ and real W , ξ , this is a damped pendulum equation.

Real periodic traveling waves of (7.28), in particular, can only occur in their stationary, standing wave guise $c = 0$; see also (1.11). The homoclinic orbit $W = \Gamma(\xi)$ of (7.28), alias a standing soliton pulse, arises in the limit of real period $p \nearrow \infty$; explicitly

$$(7.29) \quad \Gamma(\xi) = -1 + 3/\cosh^2(\xi/\sqrt{2}).$$

By now, of course, we routinely extend the pendulum ODE (7.28) to complex “time” $\zeta = \xi + i\eta$, $' = \frac{d}{d\zeta}$, and to complex $W = W(\zeta)$. As our second variant, we consider (7.28) in imaginary “time” $\zeta = i\eta$. Define $\psi(s, x) := -W(i\eta)$ in the imaginary traveling wave coordinate

$$(7.30) \quad \eta = x - cs.$$

Imaginary periods ip of $W(\zeta)$ then provide complex solutions of the scaled Schrödinger variant of (7.26), (1.16):

$$(7.31) \quad i\psi_s = \psi_{xx} + \psi^2 - 1, \quad x \in \mathbb{S}^1 = \mathbb{R}/p\mathbb{Z}.$$

The explicit standing wave (7.29) for $c = 0$, for example, possesses a minimal spatial period $p = \pi\sqrt{2}$.

For arbitrary wave speeds $c > 0$, i.e. for positive damping in (7.28), the homoclinic orbit (7.29) turns real heteroclinic, $\Gamma : -1 \rightsquigarrow +1$, from the saddle $W \equiv -1$ to the sink $W \equiv +1$. But locally, Γ is still given by the increasing part of the one-dimensional unstable manifold W^u of $W \equiv -1$. Let

$$(7.32) \quad \mu_- = \frac{1}{2}(-c + \sqrt{c^2 + 8}) > 0$$

denote the unstable real eigenvalue at $W \equiv -1$. Poincaré linearization at $W \equiv -1$, analogously to (1.19), determines the spatial period p . Explicitly,

$$(7.33) \quad p = 2\pi/\mu_- = 4\pi/(-c + \sqrt{c^2 + 8}),$$

for all $c \geq 0$. This holds near $W \equiv -1$, i.e. for real parts ξ of the analytic extension $\Gamma = \Gamma(\xi + i\eta)$ which are fixed sufficiently negative, say $\xi \leq 0$.

Fix any wave speed $c > 0$, and consider ξ as a parameter. Then the resulting family $\psi(s, x) = -\Gamma(\xi + i(x - cs))$ of rotating waves possesses fixed spatial period p and time period p/c . With respect to ξ , the family $\psi(s, x)$ is parametrized via the conjugating flow of the traveling wave equation (7.28) in real “time” $\xi \leq 0$. The parametrization of the rotating wave family reaches from small oscillations around $W \equiv -1$, at $\xi \searrow -\infty$, up to the first blow-up point, at $\xi \nearrow \min \xi^*(\eta)$. These arguments are analogous to sections 1.7, 6, and 7.3.

Specifically, the two eigenvalues μ_+ at the heteroclinic target $W \equiv +1$ of (7.28) are

$$(7.34) \quad \mu_+ = \frac{1}{2}(-c \pm \sqrt{c^2 - 8}).$$

For $c > 2\sqrt{2}$, both eigenvalues are simple, real, and stable. They are nonresonant, except for the discrete sequence of $1:m$ resonant wave speeds $c_m = \sqrt{2}(\sqrt{m} + \sqrt{1/m}) \nearrow \infty$. Nonresonant local Poincaré linearization (2.3) at the Γ -heteroclinic target $W \equiv +1$ then further aggravates the closure problem of the unstable manifold $\Gamma = W^u \setminus \{-1\}$ at the target, as we already mentioned in section 7.4.

In fact, suppose the two stable eigenvalues μ_+ are not rationally dependent, and W does not linearize to one of the two exact eigenmodes of the two stable eigenvalues μ_+ . This only discards a countable dense set of exceptional wave speeds c . For each remaining wave speed, W turns out to be 2-frequency quasi-periodic in imaginary time $\zeta = i\eta$, rather than periodic. Quasi-periodicity of $\Gamma(\xi + i\eta)$ at the target $W \equiv +1$, in imaginary time $i\eta$, implies density in a family of 2-tori, parametrized over real times ξ , and shrinking to the target equilibrium $W \equiv +1$ for $\xi \nearrow +\infty$.

For a third variant, we return to the parabolic PDE (7.26) in real time r , but for complex-valued w . Recall [GNSY13] for blow-up under Neumann boundary conditions in x . Periodic boundary conditions, instead, allow us to mix real and imaginary “time” $\zeta = \xi + i\eta$ in (7.28) and consider

$$(7.35) \quad \zeta = cr + ix.$$

Again we fix $c > 0$. The complex extension of the real heteroclinic orbit $\Gamma : -1 \rightsquigarrow +1$ of (7.28) then provides a solution $w(r, x) = -\Gamma(cr + ix)$ of the parabolic PDE (7.26). By construction and Poincaré linearization, $w(r)$ is in the PDE local unstable manifold W^u of $W \equiv -1$, for large negative r . By p -periodicity in $x = \text{Im } \zeta$, with p from (7.33), section 6 then asserts blow-up of the complex solution w in finite real time $r \nearrow \frac{1}{c} \min \xi^*(\eta)$. In the present setting, this blow-up is governed by the damped pendulum ODE (7.28). It may be interesting to pursue this construction further, and to compare the results with the approach of [GNSY13].

7.7 Ultra-invisible chaos: a 1000 € question

Even in pure ODE settings, complex time extensions of real analytic heteroclinic and homoclinic orbits Γ hold interesting promise and applied interest. We briefly sketch some recent progress. For details and many further references, we refer to [FieSch96, Fie23]. To be specific, consider rapid ε -periodic forcings g of autonomous ODE systems f , as in

$$(7.36) \quad \dot{w}(t) = f(\lambda, w(t)) + \varepsilon^p g(\lambda, \varepsilon, t/\varepsilon, w(t)).$$

The functions f, g are assumed to be analytic for small real λ, ε , all $w \in \mathbb{C}^N$, and real for real w . In the variable $\beta = t/\varepsilon$ of the rapid forcing $g = g(\lambda, \varepsilon, \beta, w)$, we only assume smoothness and period 1. Throughout, the origin $W = 0$ is assumed to be a hyperbolic equilibrium.

The time- ε stroboscope map of (7.36) may, equivalently, be seen as a one-step discretization scheme, of step size ε and order p , for the autonomous ODE

$$(7.37) \quad \dot{x} = f(\lambda, x).$$

This topic runs under the name of *backward error analysis*; see for example [BG94, Rei99, WO16] and the more detailed references in [Fie23].

Consider a nondegenerate homoclinic orbit $\Gamma : 0 \rightsquigarrow 0$ of (7.37). Here *nondegeneracy* requires that real stable and unstable manifolds of the hyperbolic equilibrium $W = 0$ cross each other at nonvanishing speed in \mathbb{R}^N , as the scalar real parameter λ increases through $\lambda = 0$. Under certain further nondegeneracy conditions on f and the perturbation g , detailed in section 5 of [FieSch96], this leads to *invisible chaos*: the chaotic region accompanying transverse homoclinics is exponentially thin, both, in parameter space (λ, ε) and along the homoclinic loop. More precisely, let

$$(7.38) \quad |s| \leq a$$

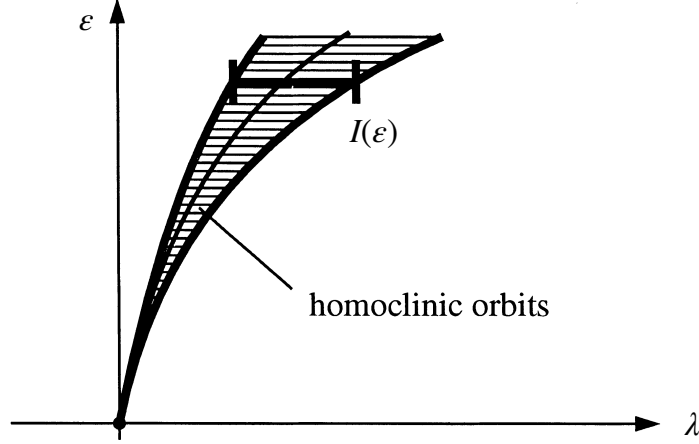


Figure 7.2: Schematic splitting region for a homoclinic orbit Γ of the ODE-flow (7.37) (hashed), under discretization with step size ε or, equivalently, under ε -periodic non-autonomous forcing (7.36); see [FieSch96]. At fixed levels of ε , the horizontal splitting intervals $\lambda \in I(\varepsilon)$ mark parameters λ for which single-round homoclinic orbits occur near Γ . For analyticity of $\Gamma(r + is)$ in a strip $|s| \leq a$, the width $\ell(\varepsilon)$ of the splitting interval $I(\varepsilon)$ is exponentially small in ε with exponent a ; see (7.39). For better visibility, the horizontal width $\ell(\varepsilon)$ of the exponentially flat splitting region has therefore been much exaggerated, in our schematic illustration. We call the dynamics in the resulting chaotic region “invisible chaos”. For complex entire homoclinic orbits $\Gamma(t)$, the exponent a could be chosen arbitrarily large. Such ultra-exponentially small splittings would lead to ultra-invisible chaos.

denote a horizontal complex strip where the complex time extension $\Gamma(r + is)$ of the real analytic homoclinic orbit $\Gamma(r)$ of (7.37) remains analytic. Then the width $\ell(\varepsilon)$ of the splitting interval $I(\varepsilon)$, where transverse homoclinicity and accompanying shift dynamics prevail, satisfies an exponential splitting estimate

$$(7.39) \quad \ell(\varepsilon) \leq C_a \exp(-a/\varepsilon),$$

for some constant $C_a > 0$ and all small $\varepsilon \rightarrow 0$. Remarkably, the splitting region is small of infinite order $\exp(-a/\varepsilon)$ in ε , even under forcings (7.36) or discretizations of finite order ε^p . See figure 7.2 for illustration. For thorough ODE surveys on this topic, going back as far as Poincaré [Poi52] and starting technically with [Nei84], see [GL01, Gel02]. For PDE extensions see [Mat01, Mat03a, MS03] and the references there.

The significance of *complex entire homoclinic orbits* Γ is now obvious. In the complex entire case, an upper estimate (7.39) would hold in any strip (7.38). In fact, we could replace (7.39) by an estimate

$$(7.40) \quad -\log \ell(\varepsilon) \geq c(1/\varepsilon) > 0,$$

for a suitable convex function c of unbounded positive slope. We would call this phenomenon *ultra-exponentially small splitting of separatrices*. Under further nondegeneracy, such splitting would be accompanied by *ultra-invisible chaos*.

Alas, can it actually happen? In [Fie23], the author has personally offered a

1,000 € reward

for settling this question.

More precisely, a *positive answer* would require any explicit example of a real nonstationary homoclinic orbit $\Gamma(t)$ to a hyperbolic equilibrium, for a complex entire ODE (7.37) on $X = \mathbb{C}^N$ with f real for real arguments, such that $\Gamma(t)$ is complex entire for $t \in \mathbb{C}$. Such an example would initiate many challenges, e.g., for numerical explorations. Eventually, it might lead towards a whole new theory to address ultra-exponentially small splitting behavior under discretization.

A *negative answer* would prove that such complex entire homoclinic orbits $\Gamma(t)$ cannot exist. For the special case of scalar second order pendulum equations

$$(7.41) \quad \ddot{w} + \mathbf{h}(w) = 0$$

with nonlinear complex entire \mathbf{h} , already Rellich [Rel40] in 1940 has most elegantly noticed the complete absence of *any* non-constant complex entire solutions $w(t)$; see also [Wit41]. Wittich has generalized this result to scalar nonautonomous m -th order equations which are a polynomial \mathbf{p} in $t, w, \dot{w}, \dots, w^{(m)}$ plus a non-polynomial complex entire nonlinearity $\mathbf{h}(w)$,

$$(7.42) \quad \mathbf{p}(w^{(m)}, \dots, w, t) + \mathbf{h}(w) = 0;$$

see [Wit50]. He requires an elementary additional condition on \mathbf{p} . His result includes the purely polynomial case $\mathbf{h} = 0$. The only complex entire solutions $w(t)$ are then polynomial in t , and hence neither homo- or heteroclinic, nor non-constant periodic. That condition is violated in our autonomous, time reversible, second order example (7.43) below, which features a periodic cosine solution (7.45).

In the general setting (7.37), entire homoclinic orbits to hyperbolic equilibria with nonresonant *real* spectrum can be excluded. See [Fie23], theorem 1.1. Resonance (1.8) is forbidden, separately, for the unstable and the stable part of the spectrum. The ODE proof is based on local Poincaré linearization (2.3), separately, in the unstable and stable manifold. Therefore the proof does not extend to the PDE case, where stable manifolds are infinite-dimensional and Poincaré linearization may fail. In the ODE case (2.3), we obtain local quasi-periodicity, in imaginary time s . For complex entire homoclinic orbits $\Gamma = \Gamma(r + is)$, we can then invoke standard results on almost periodicity [Bo32, Bes32, Cor89], and compare quasi-periodic Fourier coefficients in s , globally for large positive and negative real times r , to reach a contradiction. Our present PDE theorem 1.1 does not apply to the homoclinic case, of course, because the homoclinic target W_+ , and source $W_- = W_+$, can neither be asymptotically stable in forward time, nor backward. Cases involving complex conjugate or algebraically degenerate eigenvalues remain wide open. This includes the celebrated Shilnikov homoclinic orbits [SSTC01].

In order to protect well-established colleagues against their own, potentially intensely distracting, financial interests, the prize will be awarded to the first solution by anyone *without* a permanent position in academia. Priority is defined by submission time stamp at arxiv.org or equivalent repositories. Subsequent confirmation by regular refereed publication is required.

7.8 Non-entire homoclinic versus entire periodic orbits

Consider the time reversible, second-order, scalar ODE

$$(7.43) \quad \ddot{w} + \dot{w}^2 + w^2 - 3w = 0.$$

By integrability, the homoclinic orbit $w(t) = \Gamma(t)$ to the hyperbolic trivial equilibrium $w = 0$ satisfies

$$(7.44) \quad \frac{1}{2}\dot{w}^2 = \exp(-2w) - 1 + 2w - \frac{1}{2}w^2.$$

In particular, $\Gamma(t)$ encounters a non-meromorphic singularity in complex time. Indeed, theorem 1.1 in [Fie23] implies that Γ cannot be complex entire. The term $\exp(-2w)$ in ODE (7.44), on the other hand, prevents meromorphic singularities. If the singularity were isolated, it would therefore have to be essential.

The example (7.43) violates the condition of [Wit50] which prevents non-polynomial entire solutions. In the language of Wittich, each of the *two* terms \dot{w}^2 and w^2 is “of maximal dimension” $d = 2$, in fact, where only a single such term is permitted.

Notably, the nonlinear ODE (7.43) does possess a *complex entire* 2π -periodic orbit w given by the harmonic function

$$(7.45) \quad w(t) := 2 + \sqrt{2} \cos t.$$

Under discretizations, alias rapid forcings (7.36), such complex entire periodic orbits provide devil’s staircases with ultra-exponentially thin resonance plateaus, and correspondingly ultra-sharp Arnold tongues. See [Arn88, Dev22, GH83] for a general background. Some further details and references are discussed in section 7 of [Fie23].

Alas, our results have only provided an ultra-exponential upper estimate (7.40) for Arnold tongues associated to complex entire periodic orbits. This raises the question: how ultra-sharp are they, really? Complementary lower estimates of ultra-sharp Arnold tongues are not known. For homoclinic, rather than periodic, splittings we even lack any 1,000 € ODE example with an ultra-exponential upper estimate.

References

- [Akh90] N.I. Akhiezer. *Elements of the Theory of Elliptic Functions*. AMS Translations, Providence R.I. 1990.
- [Apo90] T.I. Apostol. *Modular Functions and Dirichlet Series in Number Theory*. Springer-Verlag, New York 1990.
- [Arn88] V.I. Arnold. *Geometrical Methods in the Theory of Ordinary Differential Equations*. Springer-Verlag, Berlin 1988.
- [BG94] G. Benettin and A. Giorgilli. On the Hamiltonian interpolation of near-to-the identity symplectic mappings with application to symplectic integration algorithms. *J. Stat. Physics* **74** (1994), 1117–1143.

- [Bes32] A.S. Besicovitch. *Almost Periodic Functions*. Cambridge University Press 1932.
- [BiZh92] J.-M. Bismut and W. Zhang. *An extension of a theorem by Cheeger and Müller. With an appendix by François Laudenbach*. Astérisque **205**, Soc. Math. de France, 1992.
- [Bo32] H. Bohr. *Fastperiodische Funktionen*. Springer-Verlag, Berlin 1932.
- [BrFie86] P. Brunovský and B. Fiedler. Numbers of zeros on invariant manifolds in reaction diffusion equations. *Nonlin. Analysis TMA* **10** (1986), 179–194.
- [BrFie88] P. Brunovský and B. Fiedler. Connecting orbits in scalar reaction diffusion equations. *Dynamics Reported* **1** (1988), 57–89.
- [BrFie89] P. Brunovský and B. Fiedler. Connecting orbits in scalar reaction diffusion equations II: The complete solution. *J. Diff. Eqns.* **81** (1989), 106–135.
- [ChIn74] N. Chafee and E. Infante. A bifurcation problem for a nonlinear parabolic equation. *J. Applic. Analysis* **4** (1974), 17–37.
- [ChVi02] V.V. Chepyzhov and M.I. Vishik. *Attractors for Equations of Mathematical Physics*. Colloq. AMS, Providence 2002.
- [COS16] C.-H. Cho, H. Okamoto, M. Shōji. A blow-up problem for a nonlinear heat equation in the complex plane of time. *Japan J. Ind. Appl. Math.* **33** (2016), 145–166.
- [CH82] S.-N. Chow and J. Hale. *Methods of Bifurcation Theory*. Springer-Verlag, New York 1982.
- [Cor89] C. Corduneanu. *Almost Periodic Functions*. With the collaboration of N. Gheorghiu and V. Barbu. Chelsea Publishing Company, New York 1989.
- [Dev22] R.L. Devaney. *An Introduction to Chaotic Dynamical Systems*. CRC Press, Boca Raton FL 2022.
- [FaKW22] M. Fasoldini, J.R. King, and J.A.C. Weideman. Blow up in a periodic semilinear heat equation. (2022); <https://arxiv.org/abs/2208.14522>
- [Fie02] B. Fiedler (ed.). *Handbook of Dynamical Systems* **2**. Elsevier, Amsterdam 2002.
- [Fie23] B. Fiedler. Real chaos and complex time. (2023); <https://arxiv.org/abs/2310.08136>
- [FieMa07] B. Fiedler, H. Matano. Blow-up shapes on fast unstable manifolds of one-dimensional reaction-diffusion equations. *J. Dyn. Differ. Eqs.* **19** (2007), 867–893.
- [FieRo14] B. Fiedler and C. Rocha. Sturm global attractors of Hamiltonian type for semilinear parabolic equations. *RIMS Kôkyûroku Bessatsu* **1881** (2014), 139–157.
- [FieRo20] B. Fiedler, C. Rocha. Boundary orders and geometry of the signed Thom-Smale complex for Sturm global attractors. *J. Dyn. Diff. Eqs.* (2020); <https://doi.org/10.1007/s10884-020-09836-5>
- [FieRo23a] B. Fiedler and C. Rocha. Design of Sturm global attractors 1: Meanders with three noses, and reversibility. *Chaos* **33**, 083127 (2023); <https://doi.org/10.1063/5.0147634>
- [FieRo24] B. Fiedler and C. Rocha. Design of Sturm global attractors 2: Time-reversible Chafee-Infante lattices of 3-nose meanders. *São Paulo J. Math. Sciences.* (2024); <https://doi.org/10.1007/s40863-023-00385-5>
- [FieRoW11] B. Fiedler, C. Rocha, and M. Wolfrum. A permutation characterization of Sturm global attractors of Hamilton type. *J. Diff. Eqs.* **252** (2011), 588–623.
- [FieSch96] B. Fiedler and J. Scheurle. *Discretization of Homoclinic Orbits, Rapid Forcing and “Invisible” Chaos*. Mem. Am. Math. Soc. **570**, Providence R.I. 1996.

- [FilMa00] M. Fila and H. Matano. Connecting equilibria by blow-up solutions. *Discrete Contin. Dyn. Syst.* **6** (2000), 155–164.
- [FilMaPo05] M. Fila, H. Matano, and P. Poláčik. Immediate regularization after blow-up. *SIAM J. Math. Anal.* **37**, No. 3, 752–776 (2005).
- [FilMi07] M. Fila and N. Mizoguchi. Multiple continuation beyond blow-up. *Differ. Integral Equ.* **20** (2007), 671–680.
- [FilPo99] M. Fila and P. Poláčik. Global solutions of a semilinear parabolic equation. *Adv. Differ. Equ.* **4** (1999), 163–196.
- [Fish1937] R.A. Fisher. The wave of advance of advantageous genes. *Ann. Eugenics* **7** (1937), 355–369.
- [For81] O. Forster. *Lectures on Riemann Surfaces*. Springer-Verlag, New York 1981.
- [Fri1916] R. Fricke. *Die elliptischen Funktionen und ihre Anwendungen. Erster Teil: Die funktionentheoretischen und analytischen Grundlagen*. Teubner, Berlin 1916. Reprint by Springer-Verlag, Heidelberg 2011.
- [GL01] V.G. Gelfreich and V.F. Lazutkin. Splitting of separatrices: perturbation theory and exponential smallness. *Russ. Math. Surv.* **56** (2001), 499–558.
- [Gel02] V.G. Gelfreich. Numerics and exponential smallness. In [Fie02] (2002), 265–312.
- [GH83] J. Guckenheimer and P. Holmes. *Nonlinear Oscillations, Dynamical Systems, and Bifurcations of Vector Fields*. Springer-Verlag, New York 1983.
- [GNSY13] J.-S. Guo, H. Ninomiya, M. Shimojo, and E. Yanagida. Convergence and blow-up of solutions for a complex-valued heat equation with a quadratic nonlinearity. *Trans. Am. Math. Soc.* **365** (2013), 2447–2467.
- [Har85] A. Haraux. A simple almost-periodicity criterion and applications. *J. Differ. Eqs.* **66** (1987), 51–61.
- [Ha88] J.K. Hale. *Asymptotic Behavior of Dissipative Systems*. Math. Surv. **25**, AMS, Providence 1988.
- [HaMO02] J.K. Hale, L.T. Magalhães, and W.M. Oliva. *Dynamics in Infinite Dimensions*. Springer-Verlag, New York 2002.
- [Har02] Ph. Hartman. *Ordinary Differential Equations*. SIAM, Providence RI 2002.
- [Hen81] D. Henry. *Geometric Theory of Semilinear Parabolic Equations*. Springer-Verlag, New York 1981.
- [IY08] Y. Ilyashenko and S. Yakovenko. *Lectures on Analytic Differential Equations*. Am. Math. Soc., Providence RI 2008.
- [Jaq21] J. Jaquette. Quasiperiodicity and blowup in integrable subsystems of nonconservative nonlinear Schrödinger equations. *J. Dyn. Differ. Eqs.* **36** (2024), 1–25. <https://doi.org/10.1007/s10884-021-10112-3>
- [JLT22a] J. Jaquette, J.-P. Lessard, A. Takayasu. Global dynamics in nonconservative nonlinear Schrödinger equations. *Adv. Math.* **398** (2022), 108234.
- [JLT22b] J. Jaquette, J.-P. Lessard, A. Takayasu. Singularities and heteroclinic connections in complex-valued evolutionary equations with a quadratic nonlinearity. *Commun. Nonlinear Sci. Numer. Simul.* **107** (2022) 106188.
- [Jo06] J. Jost. *Compact Riemann Surfaces. An Introduction to Contemporary Mathematics*. Springer-Verlag, Berlin 2006.

- [KSK17] P.G. Kevrekidis, C.I. Siettos, and Y.G. Kevrekidis. To infinity and some glimpses of beyond. *Nature Comm.* **8** (2017), 1562; <https://doi.org/10.1038/s41467-017-01502-7>
- [KPP1937] A. Kolmogoroff, I. Petrovsky, and N. Piscounoff. Étude de l'équation de la diffusion avec croissance de la quantité de matière et son application à un problème biologique. *Bull. Univ. État Moscou, Sér. Int. A: Math. et Mécan.* **1**, Fasc. 6 (1937), 1–25.
- [Ku1440] Nikolaus von Kues. *De docta ignorantia*. Bernkastel-Kues a.d. Mosel, 1440.
- [Lad91] O.A. Ladyzhenskaya. *Attractors for Semigroups and Evolution Equations*. Cambridge University Press, 1991.
- [Lam09] K. Lamotke. *Riemannsche Flächen*. Springer-Verlag, Heidelberg 2009.
- [Lan87] S. Lang. *Elliptic Functions*. Second edition. Springer-Verlag, New York 1987.
- [Lap22] P. Lappicy. Sturm attractors for fully nonlinear parabolic equations. *Rev. Mat. Complut.* **36** (2022); <https://doi.org/10.1007/s13163-022-00435-0>
- [Lap23] P. Lappicy and E. Beatriz. An energy formula for fully nonlinear degenerate parabolic equations in one spatial dimension. *Math. Ann.* (2023); <https://doi.org/10.1007/s00208-023-02740-5>
- [Mas82] K. Masuda. Blow-up of solutions of some nonlinear diffusion equations. *North-Holland Math. Stud.* **81** (1982), 119–131.
- [Mas84] K. Masuda. Analytic solutions of some nonlinear diffusion equations. *Math. Z.* **187** (1984), 61–73.
- [Mat01] K. Matthies. Time-averaging under fast periodic forcing of parabolic partial differential equations: Exponential estimates. *J. Differ. Eqs.* **174** (2001), 133–180.
- [Mat03a] K. Matthies. Exponentially small splitting of homoclinic orbits of parabolic differential equations under periodic forcing. *Discr. Contin. Dyn. Syst.* **9** (2003), 585–602.
- [MS03] K. Matthies and A. Scheel. Exponential averaging for Hamiltonian evolution equations. *Trans. Am. Math. Soc.* **355** (2003), 747–773.
- [Nei84] A.I. Neishtadt. On the separation of motions in systems with rapidly rotating phase. *J. Appl. Math. Mech.* **48** (1984), 134–139.
- [Paz83] A. Pazy. *Semigroups of Linear Operators and Applications to Partial Differential Equations*. Springer-Verlag, New York 1983.
- [Poi52] H. Poincaré. Sur le problème des trois corps et les équations de la dynamique. *Œuvres de Henri Poincaré*, Tome VII, Gauthier-Villars Paris 1952, 262–469.
- [QS19] P. Quittner and Ph. Souplet. *Superlinear Parabolic Problems. Blow-Up, Global Existence and Steady States*. 2nd ed. Birkhäuser, Cham 2019.
- [Ra02] G. Raugel. Global attractors. In [Fie02], 2002, 885–982.
- [Rei99] S. Reich. Backward error analysis for numerical integrators. *SIAM J. Numer. Analysis* **36** (1999), 1549–1570.
- [Rel40] F. Rellich. Elliptische Funktionen und die ganzen Lösungen von $y'' = f(y)$. *Math. Z.* **47** (1940), 153–160. <https://doi.org/10.1007/bf01180954>
- [San02] Stability of travelling waves. In [Fie02], 983–1055.
- [SSTC01] L.P. Shilnikov, A.L. Shilnikov, D.V. Turaev, and L.O. Chua. *Methods of Qualitative Theory in Nonlinear Dynamics. II*. World Scientific, Singapore 2001.
- [Stu17] H. Stuke. *Blow-up in Complex Time*. Dissertation Thesis, Freie Universität Berlin 2017.

- [Stu18] H. Stuke. *Complex time blow-up of the nonlinear heat equation*. (2018); <https://arxiv.org/abs/1812.10707>
- [TLJO22] A. Takayasu, J.-P. Lessard, J. Jaquette, and H. Okamoto. Rigorous numerics for nonlinear heat equations in the complex plane of time. *Numer. Math.* **151** (2022), 693–752.
- [Tan79] H. Tanabe. *Equations of Evolution*. Pitman, Boston 1979.
- [Tem88] R. Temam. *Infinite-Dimensional Dynamical Systems in Mechanics and Physics*. Springer-Verlag, New York 1988.
- [Ush80] S. Ushiki. On unstable manifolds of analytic diffeomorphisms of the plane. *RIMS Kyoto Kokyuroku* **403** (1980), 1–7.
- [Ush81] S. Ushiki. Unstable manifolds of analytic dynamical systems. *J. Math. Kyoto Univ.* **21** (1981), 763–785.
- [Wit41] H. Wittich. Ganze Lösungen der Differentialgleichung $w'' = f(w)$. *Math. Z.* **47** (1941), 422–426. <https://doi.org/10.1007/BF01180973>
- [Wol02] M. Wolfrum. Geometry of heteroclinic cascades in scalar parabolic differential equations. *J. Dyn. Diff. Eqns.* **14** (2002), 207–241.
- [Wit50] H. Wittich. Ganze transzendente Lösungen algebraischer Differentialgleichungen. *Math. Ann.* **122** (1950), 37–46. <https://doi.org/10.1007/BF01342967>
- [WO16] C. Wulff and M. Oliver. Exponentially accurate Hamiltonian embeddings of symplectic A-stable Runge-Kutta methods for Hamiltonian semilinear evolution equations. *Proc. R. Soc. Edinb. A, Math.* **146** (2016), 1265–1301.
- [Żoł06] H. Żoładek. *The Monodromy Group*. Birkhäuser, Basel 2006.